

Preprint typeset in JHEP style. - HYPER VERSION

ANL-HEP-PR-99-79
CERN-TH/99-203

The complementarity of LEP, the Tevatron and the LHC in the search for a light MSSM Higgs boson

M. Carena

*Theory Division, CERN, 1211 Geneva 23, Switzerland **
carena@fnal.gov

S. Mrenna

Physics Department, University of California at Davis, Davis, CA 95616, USA
mrenna@physics.ucdavis.edu

C.E.M. Wagner

High Energy Physics Division, Argonne National Laboratory, Argonne, IL 60439, USA †
Carlos.Wagner@cern.ch

ABSTRACT: We study the properties of the Higgs boson sector in the MSSM, putting special emphasis on radiative effects which can affect the discovery potential of the LHC, Tevatron and/or LEP colliders. We concentrate on the $Vb\bar{b}$ channel, with $V = Z$ or W , and on the channels with diphoton final states, which are the dominant ones for the search for a light Standard Model Higgs boson at LEP/Tevatron and LHC, respectively. By analyzing the regions of parameter space for which the searches in at least one of these colliders can be particularly difficult, we demonstrate the complementarity of these three colliders in the search for a light Higgs boson which couples in a relevant way to the W and Z gauge bosons (and hence plays a relevant role in the mechanism of electroweak symmetry breaking).

*On leave of absence from Fermi National Accelerator Laboratory, Batavia, IL 60510, USA

†On leave of absence from CERN, 1211 Geneva 23, Switzerland

1. Introduction

The Standard Model (SM) of particle physics provides an excellent description of data from collider experiments, including the precision electroweak observables measured at LEP and SLD. The fit to the data clearly improves if the Higgs boson has a mass less than 250 GeV [1]. LEP is the only accelerator currently running which can directly test for the existence of a Standard Model-like Higgs boson, if its mass is sufficiently light [2]. The LEP experiments at CERN have recently performed searches for a Standard Model Higgs boson at a center of mass energy of $\sqrt{s} = 189$ GeV. Preliminary limits on the Higgs mass of about 95 GeV were set by two of the experiments, DELPHI and L3. The other two experiments, ALEPH and OPAL, see a small excess of events in the mass window 90–96 GeV [3] and set an exclusion limit of about 91 GeV. LEP is currently running at a center of mass energy of 192–196 GeV and will increase gradually the center-of-mass energy towards 200 GeV and collect data until the end of the year 2000.

In spite of the phenomenological success of the SM, an explanation of the hierarchy between the Planck and the electroweak scales can only be obtained if new physics is present at scales of the order of the weak scale. The success of the SM in describing the precision electroweak data suggests (although it does not require) that any new physics should be weakly-coupled, should lead to small or negligible corrections to precision electroweak observables, and, in addition, should be consistent with a light Higgs boson. Low energy supersymmetry provides such an extension of the Standard Model.

In the minimal supersymmetric extension of the Standard Model (MSSM), the Higgs sector contains two doublets. At tree-level, the down and up quarks only couple to the neutral components of the Higgs doublet H_1 and H_2 , respectively, preventing dangerous flavor-changing neutral current (FCNC) effects. The ratio of the two Higgs doublet expectation values, v_1 and v_2 , is parametrized by $\tan\beta = v_2/v_1$. The Higgs spectrum consists of one charged, H^\pm , one CP-odd, A , and two CP-even, h and H , Higgs bosons. At tree-level all Higgs boson masses may be expressed as a function of $\tan\beta$, m_A and the W and Z boson masses, and an upper bound on the lightest CP-even Higgs mass is found, $m_h \leq M_Z |\cos 2\beta|$. This bound is modified by radiative corrections, which depend quartically on the top quark mass and logarithmically on the stop masses [4, 5, 6, 7, 8]. As will be discussed below, even after the inclusion of radiative corrections, an upper bound on the lightest CP-even Higgs mass is obtained for large values of the CP-odd Higgs mass $m_A \gtrsim 300$ GeV, for which the lightest CP-even Higgs boson has standard model-like properties.

The supersymmetric spectrum is constrained by direct experimental searches and by the requirement that it provides a good description of the precision electroweak data. This requirement implies that, unless unnatural cancellations take place [9], the soft supersymmetry-breaking mass parameter for the left-handed top-squark should

be larger than 300 GeV. Quite generally, the heavier the supersymmetric spectrum, and in particular the heavier the left-handed sfermions, the better the agreement between the MSSM and the precision electroweak observables. If supersymmetric particles are heavy, the low energy properties of the Higgs sector of the MSSM can be described by an effective theory containing two Higgs doublets, with couplings and masses fixed by the proper matching conditions at the scale of the supersymmetric particle masses.

In this low energy, effective theory, the couplings of the two CP-even Higgs bosons, h and H , to the W and Z bosons are given by the SM Higgs couplings multiplied by $\sin(\alpha - \beta)$ and $\cos(\alpha - \beta)$, respectively, where α is the Higgs mixing angle. These scaling factors are just the projections of the CP-even Higgs bosons on Φ , defined as the Higgs combination that acquires vacuum expectation value,

$$\Phi = \sqrt{2} \left[\text{Re}(H_1^0) \cos \beta + \text{Re}(H_2^0) \sin \beta \right] \equiv v + h \sin(\beta - \alpha) + H \cos(\beta - \alpha) \quad (1.1)$$

where $v \simeq 246$ GeV is the SM Higgs vacuum expectation value. In the MSSM, Φ is not a mass eigenstate. However, $\sin(\alpha - \beta)$ or $\cos(\alpha - \beta)$ becomes close to one in large regions of parameter space, reflecting the fact that one of the two Higgs bosons is mainly responsible for the electroweak symmetry breaking. In particular, for relatively large values of the CP-odd Higgs mass ($m_A \geq 300$ GeV), one finds $\sin(\alpha - \beta) \approx 1$.

The Higgs searches at LEP, the Tevatron and the Large Hadron Collider (LHC) are motivated by the desire to understand the mechanism of electroweak symmetry breaking. For this reason, it is most important to find the Higgs with relevant couplings to the W and Z bosons, with $\sin^2(\beta - \alpha)$ (or $\cos^2(\beta - \alpha)$) close to unity. For convenience, we denote such a Higgs boson as ϕ_W to emphasize its couplings to the W (and Z). As shown in Appendix A, there is a useful relation between the masses of the CP-even Higgs bosons and their couplings to the W and Z bosons,

$$m_h^2 \sin^2(\beta - \alpha) + m_H^2 \cos^2(\beta - \alpha) = m_h^2 \Big|_{m_A \gg M_Z}. \quad (1.2)$$

In Eq. (1.2), the right hand side is equal to the upper bound on the Higgs boson mass, which, for squark masses of the order of 1 TeV, is about 120–130 GeV for moderate or large values of $\tan \beta$ and about 100 GeV for $\tan \beta$ close to one [6, 10]. The above relation, Eq. (1.2), implies that the Higgs ϕ_W that couples in a relevant way to the W and Z bosons should also be relatively light, with a mass close to the upper bound when it couples to the W and Z boson with nearly SM strength. Therefore, not only is it true that the lightest CP-even Higgs boson mass is bounded from above, but, when $\cos(\beta - \alpha) \approx 1$, then the bound applies to m_H , with m_h being even smaller. If $\sin^2(\beta - \alpha) \rightarrow 1$ or $\cos^2(\beta - \alpha) \rightarrow 1$, there can be a substantial mass splitting between h and H . However, in the latter case, the mass splitting cannot be too large, or the lightest CP-even Higgs boson would have been already seen at LEP.

2. Higgs searches at present and (near) future colliders

There are three experiments that are expected to search for the Higgs ϕ_W in the mass range 95–130 GeV. LEP, at present, the Tevatron in the years 2000–2006 and LHC from 2005 on. As we mentioned above, LEP is actively looking for a Higgs boson with couplings to the Z boson and with a mass below or near 100 GeV in the channel $Z\phi_W$ with $\phi_W \rightarrow b\bar{b}$ or $\tau^+\tau^-$. If LEP reaches a center-of-mass energy of about 200 GeV and collects 200 pb⁻¹ of data per experiment, then evidence for such a Higgs boson should be observed if:

1. $\sin^2(\alpha - \beta) \simeq \mathcal{O}(1)$ (or $\cos^2(\alpha - \beta) \simeq \mathcal{O}(1)$),
2. The CP-even Higgs mass $m_h \lesssim 107$ GeV (or $m_H \lesssim 107$ GeV),
3. The branching ratio $\text{BR}(h \rightarrow b\bar{b})$ (or $\text{BR}(H \rightarrow b\bar{b})$) is close to the Standard Model value.

The Run II of the Tevatron Collider is expected to start in the year 2000. The Tevatron will have sensitivity to Higgs boson in the $V\phi$ channel, with $V = Z$ or W , and $\phi \rightarrow b\bar{b}$. Hence, its discovery potential depends also on points number 1 and 3 above, although the kinematic constraint on the Higgs mass may be relaxed (point 2). However, the Tevatron discovery potential will depend strongly on the final integrated luminosity collected by the CDF and D0 experiments [11].

Experiments at the LHC will rely mainly on the signature $pp \rightarrow \gamma\gamma + X$ to detect a Higgs ϕ_W in the mass range $m_{\phi_W} \lesssim 130$ GeV. In particular, the ATLAS and CMS experiments have performed studies that show sensitivity to ϕ_W in the channels $gg \rightarrow \phi(\rightarrow \gamma\gamma)$, $t\bar{t}\phi(\rightarrow \gamma\gamma)$, $W\phi(\rightarrow \gamma\gamma)$, and $t\bar{t}\phi(\rightarrow b\bar{b})$.¹ These studies show that these channels cover wide regions of the $m_A - \tan\beta$ plane of the MSSM, with the small m_A region ($m_A \lesssim 250$ GeV) being the most difficult. Larger coverage of the $m_A - \tan\beta$ plane in the MSSM can be achieved by considering also the production and decay signatures of all MSSM Higgs bosons [14, 15]. In these analyses, it is assumed that the sparticles have typical masses M_S of order 1 TeV, and that the stop trilinear coupling $\tilde{A}_t = A_t - \mu/\tan\beta$ is much smaller than M_S . The latter is, in principle, a conservative assumption, since, for low luminosity, and for a Higgs mass $m_{\phi_W} \leq 130$ GeV, the reach potential improves for larger values of the Higgs mass

¹Several other channels have been proposed which would be useful for studying a Higgs boson with SM-like couplings to the gauge bosons and up-quarks[12, 13]. However, these are experimentally challenging, and, to the best of our knowledge, the ATLAS and CMS collaborations have not yet analyzed the reach in these channels. We shall therefore not discuss these channels in detail, although we shall analyze their possible relevance in sections 3 and 4.3.

(large values of \tilde{A}_t , M_S , etc.). In the present study, we are interested in the search for ϕ_W and we shall hence concentrate on only its signatures.

The object of the present study is to illustrate the relationship between measurements at the different colliders, and to demonstrate the potential of the combined experimental program to discover the Higgs ϕ_W . In the following section, we will review the behavior of the Higgs boson couplings to particles and sparticles with respect to variations in the MSSM parameters. In particular, we will show their impact on production cross sections and branching ratios. Given the sensitivity of the various experiments to discover a Higgs boson as a function of the Higgs boson mass and their integrated luminosity, we then calculate the corresponding sensitivity in the MSSM, based on the Standard Model experimental simulations done at the LEP, Tevatron and LHC colliders.² This will be shown in Section 4. We pay particular attention to choices of MSSM parameters which will clearly lead to difficulty at one of the experiments, and explain why this increases the sensitivity of the complementary experiment. Our conclusions are stated in Section 5.

3. The couplings of the CP-even Higgs bosons

Quite generally, the two CP-even Higgs boson eigenstates are a mixture of the real, neutral components of the H_1 and H_2 Higgs doublets,

$$\begin{pmatrix} h \\ H \end{pmatrix} = \begin{pmatrix} -\sin \alpha & \cos \alpha \\ \cos \alpha & \sin \alpha \end{pmatrix} \begin{pmatrix} \sqrt{2}Re(H_1^0) - v_1 \\ \sqrt{2}Re(H_2^0) - v_2 \end{pmatrix}, \quad (3.1)$$

and the lightest CP-even Higgs boson couples to down quarks/leptons and up quarks by its Standard Model values times $-\sin \alpha / \cos \beta$ and $\cos \alpha / \sin \beta$, respectively. The couplings to the heavier CP-even Higgs boson are given by the standard model values times $\cos \alpha / \cos \beta$ and $\sin \alpha / \sin \beta$, respectively. Analogously, the coupling of the CP-odd Higgs boson to down quarks/leptons and up quarks is given by the Standard Model coupling times $\tan \beta$ and $1 / \tan \beta$, respectively. The lightest (heaviest) CP-even Higgs boson has VVh (VVH) couplings which are given by the Standard Model value times $\sin(\beta - \alpha)$ ($\cos(\beta - \alpha)$), where V represents a W or Z boson. The coupling of a CP-even and a CP-odd Higgs boson with a Z boson ZhA (ZHA) is proportional to $\cos(\beta - \alpha)$ ($\sin(\beta - \alpha)$).

As stated above, LEP is presently exploring the Higgs mass region 95 GeV $\lesssim m_{\phi_W} \lesssim 107$ GeV. Already the present bounds on a SM-like Higgs mass, of about 95 GeV, put strong constraints on the realization of the infrared fixed-point scenario

²The sensitivity or R -value is the ratio of the Higgs production cross section times Higgs decay branching ratio to the ones necessary to claim discovery in the Standard Model. If $R > 1$, then an enhancement of the Higgs production rate and/or branching ratio over the Standard Model expectation is needed to claim discovery for a stated luminosity. If $R < 1$, then the Standard Model Higgs boson can be discovered with less luminosity.

in the MSSM, and, in general, of the small $\tan\beta$ scenario, with $\tan\beta$ close to one [10]. Indeed, if a SM-like Higgs were discovered at LEP in this region of mass, the fixed-point scenario could only be accommodated for large values of the stop masses and of the stop mixing parameters. In general, this Higgs ϕ_W mass range is naturally obtained for $2 < \tan\beta \lesssim 5$, with smaller values of the Higgs mass being obtained for smaller values of $\tan\beta$. Larger values of the ratio of Higgs vacuum expectation values, $\tan\beta > 5$, tend to lead to values of the Higgs ϕ_W mass beyond the reach of LEP. It is important to stress that, in the presence of large mixing in the lepton sector, as suggested by the SuperKamiokande data, these values of $\tan\beta$, $2 < \tan\beta \lesssim 5$, are consistent with the unification of the bottom and τ Yukawa couplings at the grand unification scale [16].

As explained above, the present experimental constraints are most naturally satisfied for moderate or large values of $\tan\beta$, $\tan\beta > 2$. For $\tan\beta$ larger than a few, the approximation $\sin\beta \simeq 1$, and hence, $1/\cos\beta \simeq \tan\beta$, is a good one, and one can construct the following table of simplified *tree level* couplings of fermions and gauge bosons ($V \equiv W$ or Z) to the CP-even Higgs bosons relative to their Standard Model values:

	$b\bar{b}$	$t\bar{t}$	VV	
h	$-\sin\alpha \times \tan\beta$	$\cos\alpha$	$\cos\alpha$	
H	$\cos\alpha \times \tan\beta$	$\sin\alpha$	$\sin\alpha$	(3.2)

Note that the tree level couplings $t\bar{t}\phi$ and $VV\phi$ exhibit the same behavior, so that, for the same values of the Higgs mass the production rates for $Z\phi$ at LEP, $W/Z\phi$ at the Tevatron, and $t\bar{t}/W\phi$ at the LHC are simultaneously enhanced or suppressed with respect to the Standard Model case. Also, for heavy sparticles, the $\phi \rightarrow gg$ decay rate (which determines the $gg \rightarrow \phi$ production rate) is approximately proportional to the tree level $t\bar{t}\phi$ coupling. Therefore, the production of $t\bar{t}\phi$, $W\phi$ and $gg \rightarrow \phi$ have the same dependence on the MSSM couplings (when the sparticles are heavy). Moreover, when sparticles are heavy, the partial width for the decay of the Higgs boson to a photon pair depends on one-loop contributions from the top quark and W boson, which come with opposite signs. When the sparticles are light, however, all color-charged sparticles affect the ϕgg coupling, while all electrically-charged sparticles affect the $\phi\gamma\gamma$ coupling, and we will show a few examples in which their effect become relevant. Finally, it is important to remark that, while for $\tan\beta$ larger than a few, the $t\bar{t}\phi$ and $VV\phi$ couplings depend only weakly on $\tan\beta$, the $\phi b\bar{b}$ coupling has a strong dependence on this parameter, and may be strongly affected by radiative corrections proportional to $\tan\beta$ [17, 18]. This can have a significant impact on Higgs decay branching ratios.

The LEP experiments are sensitive to the Higgs ϕ_W mainly through the $Z\phi(\rightarrow b\bar{b})$ process. Given the cross section limit for the Standard Model Higgs boson, the MSSM limit is derived by properly including the MSSM couplings. Figure 1 shows

the reach of the Standard Model Higgs discovery potential of the LEP and Tevatron colliders for different integrated luminosities of the latter as a function of R , defined as the total $Vb\bar{b}$ production rate normalized to the Standard Model value:

$$R(m_\phi) = \frac{\sigma(V\phi) \text{BR}(\phi \rightarrow b\bar{b})}{\sigma(V\phi)_{SM} \text{BR}(\phi \rightarrow b\bar{b})_{SM}}. \quad (3.3)$$

The subscript SM in Eq. (3.3) denotes the Standard Model values. For the case of the MSSM, the production cross section is only modified by the strength of the $VV\phi$ coupling, so that

$$\begin{aligned} R(m_\phi) &= \left\{ \sin^2(\beta - \alpha), \cos^2(\beta - \alpha) \right\} \frac{\text{BR}(\phi \rightarrow b\bar{b})}{\text{BR}(\phi \rightarrow b\bar{b})_{SM}} \\ &\simeq \left\{ \cos^2 \alpha, \sin^2 \alpha \right\} \frac{\text{BR}(\phi \rightarrow b\bar{b})}{\text{BR}(\phi \rightarrow b\bar{b})_{SM}}, \end{aligned} \quad (3.4)$$

where the left (right) portion of the expression in brackets refers to $\phi = h(H)$, and we have used the approximations of Table I in the second line. If R is too small, then discovery of a SM-like Higgs boson will not be possible. Problem regions are when: (a) $h \equiv \phi_W$ or $H \equiv \phi_W$ but m_h or m_H is too large to be kinematically accessible, (b) h (H) has SM-like couplings to the gauge bosons, but $\text{BR}(\phi_W \rightarrow b\bar{b})$ is suppressed because the mixing angle α is such that $\sin \alpha / \cos \beta \ll 1$ ($\cos \alpha / \cos \beta \ll 1$) or because there are large radiative corrections, induced by supersymmetric particles, which lead to a suppression of the renormalized $\phi_W b\bar{b}$ coupling, and (c) $\cos^2(\beta - \alpha) \simeq \sin^2(\beta - \alpha)$ and m_h and m_H are sufficiently different in mass, so that the production cross section for both Higgs bosons is small and the two signals do not overlap. The experiments in Run II and Run III (the proposed high-luminosity run) at the Tevatron are sensitive to both the $W\phi(\rightarrow b\bar{b})$ and $Z\phi(\rightarrow b\bar{b})$ processes. Since these depend on the same couplings, the previous discussion for LEP holds, except that (a) will not occur provided the experiments receive *enough integrated luminosity*.

As stated above, the $\phi b\bar{b}$ coupling can become small because a tree level coupling vanishes or because of large radiative corrections. The former occurs when $\sin \alpha$ or $\cos \alpha$ vanishes, whereas, as explained below, the latter depends on the soft supersymmetry-breaking parameters, but tends to occur for small values of $\sin \alpha$ or $\cos \alpha$, such that the tree level coupling is non-vanishing, but still suppressed compared to the SM one. The value of α is determined by diagonalizing the quadratic mass matrix \mathcal{M}^2 for the CP-even Higgs bosons:

$$\mathcal{M}^2 = \begin{pmatrix} \mathcal{M}_{11}^2 & \mathcal{M}_{12}^2 \\ \mathcal{M}_{12}^2 & \mathcal{M}_{22}^2 \end{pmatrix}, \quad (3.5)$$

where the matrix components are given by [6, 18]

$$\mathcal{M}_{11}^2 \simeq m_A^2 \sin^2 \beta + M_Z^2 \cos^2 \beta$$

$$\begin{aligned}
& - \frac{h_t^4 v^2}{16\pi^2} \bar{\mu}^2 \sin^2 \beta \tilde{a}^2 \left[1 + \frac{t}{16\pi^2} (6h_t^2 - 2h_b^2 - 16g_3^2) \right] + \mathcal{O}(h_t^2 M_Z^2) \\
& - \frac{h_b^4 v^2}{16\pi^2} \bar{\mu}^2 \sin^2 \beta \bar{A}_b^2 \left[1 + \frac{t}{16\pi^2} (6h_b^2 - 2h_t^2 - 16g_3^2) \right] \\
\mathcal{M}_{22}^2 & \simeq m_A^2 \cos^2 \beta + M_Z^2 \sin^2 \beta \left(1 - \frac{3}{8\pi^2} h_t^2 t \right) \\
& + \frac{h_t^4 v^2}{16\pi^2} 12 \sin^2 \beta \left\{ t \left[1 + \frac{t}{16\pi^2} (1.5h_t^2 + 0.5h_b^2 - 8g_3^2) \right] \right. \\
& + \bar{A}_t \tilde{a} \left(1 - \frac{\bar{A}_t \tilde{a}}{12} \right) \left[1 + \frac{t}{16\pi^2} (3h_t^2 + h_b^2 - 16g_3^2) \right] \left. \right\} \\
& - \frac{v^2 h_b^4}{16\pi^2} \sin^2 \beta \bar{\mu}^4 \left[1 + \frac{t}{16\pi^2} (9h_b^2 - 5h_t^2 - 16g_3^2) \right] + \mathcal{O}(h_t^2 M_Z^2) \\
\mathcal{M}_{12}^2 & \simeq - \left[m_A^2 + M_Z^2 - \frac{h_t^4 v^2}{8\pi^2} (3\bar{\mu}^2 - \bar{\mu}^2 \bar{A}_t^2) \right] \sin \beta \cos \beta \\
& + \left[\frac{h_t^4 v^2}{16\pi^2} \sin^2 \beta \bar{\mu} \tilde{a} [\bar{A}_t \tilde{a} - 6] + \frac{3h_t^2 M_Z^2}{32\pi^2} \bar{\mu} \tilde{a} \right] \left[1 + \frac{t}{16\pi^2} (4.5h_t^2 - 0.5h_b^2 - 16g_3^2) \right] \\
& + \frac{h_b^4 v^2}{16\pi^2} \sin^2 \beta \bar{\mu}^3 \bar{A}_b \left[1 + \frac{t}{16\pi^2} (7.5h_b^2 - 3.5h_t^2 - 16g_3^2) \right]. \tag{3.6}
\end{aligned}$$

In Eq. (3.6), g_3 is the QCD running coupling constant, h_t and h_b are the top and bottom Yukawa couplings, and the barred quantities (e.g. \bar{A}_t) are the usual MSSM parameters divided by the SUSY scale M_S . The quantity $\tilde{a} \equiv \bar{A}_t - \bar{\mu}/\tan\beta$ and $t = \ln(M_S^2/m_t^2)$. Only the leading terms in powers of h_b and $\tan\beta$ have been retained, and the small, $\mathcal{O}(h_t^2 M_Z^2)$ correction to \mathcal{M}_{12}^2 has been explicitly included. Note, the above expressions hold only in the limit of small splittings between the running stop masses, and the condition $2m_t \max(|A_t|, |\mu|) < M_S^2$ must be fulfilled, with a similar condition in the sbottom sector. The analytical expressions presented above are very useful, since they provide an understanding of the behavior of the Higgs masses and mixing angles with the stop and sbottom soft supersymmetry breaking masses and mixing parameters, and, unless the stop and sbottom mass splittings are very large, they provide an excellent approximation to the precise Higgs mass matrix elements. However, the final, numerical results of our analysis make use of the complete one-loop RG improved effective potential computation [6] of the Higgs squared mass matrix elements, which allows a more reliable treatment of the cases in which the squark mixing terms or the squark mass splittings become large.

The approximation that $\sin\beta \simeq 1$, which is good for moderate or large values of $\tan\beta$, is equivalent to the relation $v_2^2 \gg v_1^2$. In this limit, H_2 is the Higgs doublet mainly responsible for electroweak symmetry breaking and the mass of the Higgs ϕ_W is well approximated by $\sqrt{\mathcal{M}_{22}^2}$, where the m_A dependence is suppressed by the large $\tan\beta$ factor. On the other hand, the mixing angle α can be determined from the

expression

$$\sin \alpha \cos \alpha = \frac{\mathcal{M}_{12}^2}{\sqrt{(\text{Tr} \mathcal{M}^2)^2 - 4 \det \mathcal{M}^2}}. \quad (3.7)$$

In the limit that $\mathcal{M}_{12} \rightarrow 0$, either $\sin \alpha$ or $\cos \alpha \rightarrow 0$. In the case that $\mathcal{M}_{11}^2 > \mathcal{M}_{22}^2$, it is $\sin \alpha$ that vanishes. Otherwise, it is $\cos \alpha$ that vanishes. Because $\mathcal{M}_{11}^2 \simeq m_A^2 \sin^2 \beta \simeq m_A^2$, it is $\sin \alpha$ that is suppressed when the off-diagonal elements of the quadratic mass matrix are small and m_A is large. In both cases the suppression of the BR($\phi \rightarrow b\bar{b}$) affects the Higgs ϕ_W . Observe that the tree-level contribution to the Higgs matrix element \mathcal{M}_{12}^2 is suppressed by a $1/\tan \beta$ factor. This factor does not lead in general to a suppression of the effective ϕ_W coupling to bottom quarks, but compensates the $\tan \beta$ enhancement of h_b to render it Standard Model-like. What is emphasized above is an additional suppression, which only takes place when \mathcal{M}_{12}^2 is significantly smaller than the tree level value. In general, the radiative corrections are very important and depend on the sign and size of $\bar{\mu} \times \bar{A}_t$ and $\bar{\mu} \times \bar{A}_b$. The possibility of such effects will no be apparent if one assumes $\mu \simeq 0$ or $A_t, A_b \simeq 0$.

Up to this point, the discussion has made use of the tree-level (but QCD corrected) relation between the Yukawa couplings and the quark masses. However, for large values of $\tan \beta$, there can be a significant modification of the bottom and possibly tau Yukawa couplings from SUSY corrections [17, 18]. In fact, it is possible to enhance the bottom or tau coupling of the Higgs boson independently of each other. For completeness, we provide the modifications to the $\phi b\bar{b}$ couplings derived by us earlier ³ in an effective Lagrangian approach [18]. The starting point is the effective Lagrangian at energies below the supersymmetric particle masses, which are assumed to be larger than the weak scale, $M_S^2 \gg M_Z^2$,

$$\mathcal{L} \simeq h_b H_1^0 b\bar{b} + \Delta h_b H_2^0 b\bar{b}. \quad (3.8)$$

In the above, the appearance of the one-loop suppressed coupling Δh_b is a reflection of the breakdown of supersymmetry at low energies. The CP-even Higgs boson couplings to bottom quarks are approximately given by [18]

$$h_{b,h} \simeq -\frac{m_b \sin \alpha}{v \cos \beta} \left[1 - \frac{\Delta(m_b)}{1 + \Delta(m_b)} \left(1 + \frac{1}{\tan \alpha \tan \beta} \right) \right], \quad (3.9)$$

$$h_{b,H} \simeq \frac{m_b \cos \alpha}{v \cos \beta} \left[1 - \frac{\Delta(m_b)}{1 + \Delta(m_b)} \left(1 - \frac{\tan \alpha}{\tan \beta} \right) \right], \quad (3.10)$$

where $h_{b,h}$ and $h_{b,H}$ denote the couplings of the lightest and heaviest CP-even Higgs

³These results agree with those obtained by diagrammatic computations[19, 20].

boson respectively and $\Delta(m_b) = (\Delta h_b/h_b) \tan \beta$. The coupling of the CP-odd Higgs boson is much simpler, and takes the form

$$h_{b,A} = \frac{m_b}{(1 + \Delta(m_b))v} \tan \beta \simeq h_b. \quad (3.11)$$

The function $\Delta(m_b)$ contains two main contributions, one from a bottom squark–gluino loop (depending on the two bottom squark masses $M_{\tilde{b}_1}$ and $M_{\tilde{b}_2}$ and the gluino mass $M_{\tilde{g}}$) and another one from a top squark–higgsino loop (depending on the two top squark masses $M_{\tilde{t}_1}$ and $M_{\tilde{t}_2}$ and the higgsino mass parameter μ). The explicit form of $\Delta(m_b)$ at one-loop can be approximated by computing the supersymmetric loop diagrams at zero external momentum ($M_S \gg m_b$) and is given by [21, 22, 23, 24]:

$$\Delta(m_b) \simeq \frac{2\alpha_3}{3\pi} M_{\tilde{g}} \mu \tan \beta I(M_{\tilde{b}_1}, M_{\tilde{b}_2}, M_{\tilde{g}}) + \frac{Y_t}{4\pi} A_t \mu \tan \beta I(M_{\tilde{t}_1}, M_{\tilde{t}_2}, \mu), \quad (3.12)$$

where $\alpha_3 = g_3^2/4\pi$, $Y_t = \frac{h_t^2}{4\pi}$, and the function I is given by,

$$I(a, b, c) = \frac{a^2 b^2 \ln(a^2/b^2) + b^2 c^2 \ln(b^2/c^2) + c^2 a^2 \ln(c^2/a^2)}{(a^2 - b^2)(b^2 - c^2)(a^2 - c^2)}, \quad (3.13)$$

which is positive by definition. Smaller contributions to $\Delta(m_b)$ [23] have been neglected for the purpose of this discussion. The value of $\Delta(m_b)$ in Eq. (3.12) is defined at the scale M_S , where the sparticles are decoupled. The h_b and Δh_b couplings should be computed at that scale, and run down with their respective renormalization group equations to the scale m_A , where the relations between the couplings of the bottom quark to the neutral Higgs bosons and the running bottom quark mass are defined.

The CP-even Higgs couplings to the τ -leptons are also affected by large corrections at large $\tan \beta$. They are given by similar expressions as the ones for the bottom couplings, but replacing $\Delta(m_b)$ by

$$\Delta(m_\tau) \simeq \frac{g_1^2}{16\pi^2} M_1 \mu \tan \beta I(M_{\tilde{\tau}_1}, M_{\tilde{\tau}_2}, M_1) + \frac{g_2^2}{16\pi^2} M_2 \mu \tan \beta I(M_{\tilde{\nu}_\tau}, M_2, \mu), \quad (3.14)$$

where g_1 and g_2 are the $U(1)$ hypercharge and $SU(2)$ weak isospin couplings. Since it is proportional to weak couplings, $\Delta(m_\tau)$ is usually much smaller than $\Delta(m_b)$; the exact value of $\Delta(m_\tau)$ depending on the relative size of the weak gaugino masses.

In the earlier discussion of the suppression of the $\phi b\bar{b}$ coupling, an implicit assumption was made that $\Delta(m_b)$ and $\Delta(m_\tau)$ were small. Indeed, from Eq. (3.9) (Eq. (3.10)), we observe that, in the limit $\sin \alpha = 0$ ($\cos \alpha = 0$), the $\phi b\bar{b}$ coupling is given by

$$h_{b,h}(h_{b,H}) = \frac{m_b}{\sin \beta v} \times \frac{\Delta(m_b)}{(1 + \Delta(m_b))} \equiv \Delta h_b, \quad (3.15)$$

which vanishes if $|\Delta(m_b)| \ll 1$. A similar expression to Eq. (3.15) holds for the τ lepton coupling.

The bottom mass correction factor $\Delta(m_b) \ll 1$, except when $\tan\beta$ and/or the stop mixing mass parameters A_t and μ are large, in which case it can be near unity. When $\Delta(m_b)$ is of order 1, the $\phi b\bar{b}$ coupling can be of the order of the Standard Model one even though $\sin\alpha \cos\alpha \rightarrow 0$. Moreover, since $\Delta(m_b)$ and $\Delta(m_\tau)$ will be different in general, their relative strength can be quite different from that in the SM or the tree-level MSSM. It is possible for $h_{\tau,h}$ to vanish, while $h_{b,h}$ is substantial. Note, a strong suppression of the bottom coupling $h_{b,h}$ can still occur for slightly different values of the Higgs mixing angle α , namely

$$\tan\alpha \simeq \frac{\Delta(m_b)}{\tan\beta} \equiv \frac{\Delta h_b}{h_b}. \quad (3.16)$$

Under these conditions,

$$h_{\tau,h} = \frac{m_\tau}{v \sin\beta} \left(\frac{\Delta(m_\tau) - \Delta(m_b)}{1 + \Delta(m_\tau)} \right), \quad h_{b,h} = 0. \quad (3.17)$$

A similar expression is obtained for the coupling $h_{\tau,H}$ in the case $h_{b,H} = 0$. Hence, if $\tan\beta$ is very large and $\Delta(m_b)$ is of order one, the τ Yukawa coupling may *not* be strongly suppressed with respect to the Standard Model case and can provide the *dominant* decay mode for a Standard Model-like Higgs boson. Likewise, a suppression of the $h_{\tau,h}$ coupling arises for $\tan\alpha \simeq \Delta(m_\tau)/\tan\beta$.

At tree-level, when $\phi \rightarrow b\bar{b}$ vanishes, so does $\phi \rightarrow \tau^+\tau^-$. Therefore, the Higgs decays to $gg, c\bar{c}, W^*W^*$ and $\gamma\gamma$ occur at enhanced rates compared to the SM expectations. Once the vertex corrections are included, the results will depend on $\Delta(m_b)$ (we assume for the rest of this discussion that $\Delta(m_\tau)$ is small). Since the $\Delta(m_b)$ corrections depend strongly on the size and sign of $M_{\tilde{g}}$, and hence introduce a dependence on parameters which do not otherwise affect the Higgs masses and mixing angles in a relevant way, we shall neglect them in the main analysis. However, in Section 4, we shall present a dedicated analysis of the possible effects of these corrections on the Higgs phenomenology.

The vanishing of the $\phi b\bar{b}$ coupling may be problematic for Higgs searches at LEP and the Tevatron. The enhanced decays $\phi \rightarrow gg$ and $\phi \rightarrow c\bar{c}$ are difficult to observe at the LEP and particularly at the Tevatron collider because of increased backgrounds. The ‘‘trilepton’’ signature from $W\phi(\rightarrow W^*W^*)$ may be challenging at the Tevatron [25], because of the small signal rate. While the cross section for the process $gg \rightarrow \phi \rightarrow \gamma\gamma$ can be enhanced up to about 10 fb at the Tevatron collider, which may be observable, a detailed study of the $\gamma\gamma$ backgrounds in the mass range around 100 GeV is still lacking.

We now turn our attention to the case of the LHC. Search strategies in the $\gamma\gamma + X$ final state change from the low luminosity run (collecting up to 30 fb^{-1}) to

the high luminosity run (30 to 100 fb⁻¹ and up to 300 fb⁻¹)⁴ because of the relative behavior of the signals and backgrounds. At low luminosity, the experiments are most sensitive to the subprocess $gg \rightarrow \phi \rightarrow \gamma\gamma$. Given the reach for a SM Higgs boson, the reach in the MSSM can be calculated using the factor $R'(m_\phi)$:

$$R'(m_\phi) = \frac{\Gamma(\phi \rightarrow gg) \text{BR}(\phi \rightarrow \gamma\gamma)}{\Gamma(\phi \rightarrow gg)_{SM} \text{BR}(\phi \rightarrow \gamma\gamma)_{SM}}. \quad (3.18)$$

At high luminosity, the best reach for a Higgs with SM-like couplings to the gauge bosons is in the $W\phi_W(\rightarrow \gamma\gamma)$ and $t\bar{t}\phi_W(\rightarrow \gamma\gamma)$ channels. In this case, the production cross section depends on a tree level coupling, and loop effects arise only in $\text{BR}(\phi_W \rightarrow \gamma\gamma)$. The relevant factor $R''(m_\phi)$ is

$$\begin{aligned} R''(m_\phi) &= \left\{ \sin^2(\beta - \alpha), \cos^2(\beta - \alpha) \right\} \frac{\text{BR}(\phi \rightarrow \gamma\gamma)}{\text{BR}(\phi \rightarrow \gamma\gamma)_{SM}} \\ &\simeq \left\{ \cos^2 \alpha, \sin^2 \alpha \right\} \frac{\text{BR}(\phi \rightarrow \gamma\gamma)}{\text{BR}(\phi \rightarrow \gamma\gamma)_{SM}}. \end{aligned} \quad (3.19)$$

Let us analyze the properties of the Higgs sector relevant to R' and R'' in more detail. The effect of a light top squark (or light bottom squark at large $\tan\beta$) with \tilde{A}_t ($\tilde{A}_b \equiv A_b - \mu \tan\beta$) large is to decrease the top quark contribution to these loop effects. This decreases the partial width $\Gamma(\phi_W \rightarrow gg)$, but increases $\text{BR}(\phi_W \rightarrow \gamma\gamma)$ since in the Standard Model the W and t contributions destructively interfere, with the former being the dominant one. It was noted earlier that there is a reciprocal relation between $\Gamma(\phi_W \rightarrow gg)$ and $\Gamma(\phi_W \rightarrow \gamma\gamma)$ because of the domination of the WW loop in the latter [26]. Because $\text{BR}(\phi_W \rightarrow \gamma\gamma) = \Gamma(\phi_W \rightarrow \gamma\gamma)/\Gamma_{tot}$, the relation is not entirely compensating, since $\text{BR}(\phi_W \rightarrow \gamma\gamma)$ depends on Γ_{tot} and hence on the width of the Higgs decay into bottom quarks and tau leptons. For small values of $\tan\beta$ or large values, the factor R' , Eq. (3.18) can be significantly decreased [26] because of a cancellation between the top quark loops and the stop and sbottom loops. Of course, the presence of light sparticles implies that the next generation of experiments can directly probe them. The advantage of the $t\bar{t}\phi_W$ channel is that R'' depends on $\text{BR}(\phi_W \rightarrow \gamma\gamma)$ and not $\Gamma(\phi_W \rightarrow gg)$. Therefore, the decrease in R' can be compensated by an increase in R'' .

Another way to modify R' and R'' is to change one of the tree level couplings listed above. For instance, when $\tan\beta$ is large and $\sin\alpha$ is small, the lightest CP-even Higgs boson presents Standard Model-like couplings to the W and Z gauge bosons. However, even when $\sin\alpha$ is small, the product $\sin\alpha \times \tan\beta$ is not determined a priori, and depends on the exact characteristics of the supersymmetric spectrum. When $\sin\alpha \times \tan\beta$ is larger than one, the $\text{BR}(h \rightarrow b\bar{b})$ becomes larger than the SM one,

⁴We use the term luminosity interchangeably to mean instantaneous luminosity and total integrated luminosity. The meaning should be clear from context.

and, since it is the dominant Higgs decay channel, it partially suppresses the $\text{BR}(\phi \rightarrow \gamma\gamma)$. On the contrary, if $\text{BR}(h \rightarrow b\bar{b})$ becomes much smaller than one, something that, as we explained above, can happen in certain regions of parameters [18], the $\text{BR}(\phi \rightarrow \gamma\gamma)$ will be strongly enhanced, improving the LHC prospects of finding a light CP-even Higgs without going to the highest luminosity runs.

Our discussion of searches for a SM-like Higgs boson at the LHC is limited to those presented by the experiments themselves. ATLAS has presented encouraging numbers for their reach in the $t\bar{t}\phi(\rightarrow b\bar{b})$ channel.⁵ In the approximation of Table I, we observe that this signature has large or small couplings in the same regions of MSSM parameters space as for $V\phi(\rightarrow b\bar{b})$ at the LEP and Tevatron colliders. This potentially important channel is not included in our analysis. Let us mention, however, that, if the Higgs were discovered at LEP and/or the Tevatron, this channel will serve to measure its coupling to the top quark, providing an important independent test of the origin of fermion masses. On the other hand, if the effective luminosity at the next run of the Tevatron were small, this channel will provide additional means for the LHC to test the Higgs responsible for electroweak symmetry breaking in most of the MSSM parameter space. Hence, this Higgs production channel at LHC adds to the complementary physics potential of the three colliders that we are emphasizing in this article.

4. Results

For our analysis, we rely on the projected discovery reach of the three colliders for a Standard Model Higgs boson. For LEP2, running at $\sqrt{s} = 200$ GeV and collecting 200 pb^{-1} of data (per experiment), we use the numbers of Ref. [27]. For the Tevatron in Run II and Run III, we use the results of the Higgs Working Group of the Workshop on Physics at Run II [11]. For the LHC, we use the technical design reports and updates of the ATLAS[14] and CMS[15] collaborations. A comparison of the sensitivity of the two experiments in the $\gamma\gamma$ channels reveals that CMS is substantially more sensitive than ATLAS. Therefore, only the projected reach of the CMS detector is explicitly used in our analysis to represent the reach of the LHC. To demonstrate the potential of the LHC if 300 fb^{-1} of data is collected, we scale the 100 fb^{-1} significances by a factor of $\sqrt{3}$. The significance in the MSSM is determined by rescaling the partial widths and branching ratios accordingly.

As discussed in Sec. 3, some choices for the soft supersymmetry-breaking parameters at the weak scale can make it difficult to observe the Higgs ϕ_W at LEP and the Tevatron in the $\phi_W \rightarrow b\bar{b}$ channel or LHC in the $\phi_W \rightarrow \gamma\gamma$ channel. In this section, we demonstrate that, quite generally, difficulties will not arise in *both* chan-

⁵At low luminosity, the process $W\phi(\rightarrow b\bar{b})$ can also be used.

nels, provided that the experiments operate efficiently and receive enough integrated luminosity.

We construct our argument by concentrating on MSSM parameters that are problematic for one of the channels, and then displaying the complementarity of the other channel. Our choices include the possibility of light top and bottom squarks, which can have an important impact on one-loop suppressed decays of ϕ_W . Higgs boson properties are calculated using HDECAY [28]. However, due to the relevance of the bottom mass corrections in defining the proper bottom quark Yukawa coupling at the scale M_S , we have modified the effective potential calculation of Ref. [6], used in HDECAY, in order to include these corrections in the large $\tan\beta$ regime. The inclusion of these corrections in the expression of the Higgs masses lead to non-leading logarithmic two-loop corrections. Although in a complete two-loop calculation there might be other non-logarithmic terms modifying the Higgs masses, these corrections are particularly important, since they can modify the one-loop result by factors of order one.

4.1 The Minimal Mixing Model

The case when $\tilde{A}_t = 0$ yields the smallest value for the upper bound on the Higgs boson mass for a given choice of μ and stop masses (for large values of $\tan\beta$, small sbottom masses or large values of μ tend to lead to even lower values for the upper bound [6]). We fix the overall scale of supersymmetry particle masses $M_S = 1$ TeV, with $M_S^2 = \frac{1}{2}(m_{\tilde{t}_1}^2 + m_{\tilde{t}_2}^2)$. Furthermore, for comparison with the results presented by ATLAS and CMS, we choose $\mu = -100$ GeV, which is small enough that it does not differ significantly from the $\mu = 0$ case, but large enough to avoid a light chargino. In our scan of the $m_A - \tan\beta$ plane, we tune $A_t = \mu/\tan\beta$ to achieve the conditions of minimal mixing at each point in the plane. This choice of parameters yields a moderate upper bound for the lightest Higgs boson mass which is, however, beyond the kinematic reach of LEP. This is a conservative assumption for the LHC experiments, since the discovery reach is typically best for a Higgs ϕ_W mass near the highest allowed upper bound in the MSSM.

The regions of the $M_A - \tan\beta$ plane in which a Higgs ϕ_W boson would be discovered at the 5- σ level at the Tevatron are shown as shaded regions in Fig. 2(a). Different shadings correspond to different assumptions about the luminosity delivered to *both* experiments. The LEP discovery contour (for a Higgs ϕ_W boson) is shown by the double line (the region below the contour will be probed). With *more* than 5 fb⁻¹, the Tevatron begins to provide information beyond that from LEP, provided that the Higgs boson is not already discovered. Up to 30 fb⁻¹ of data is needed to cover the problematic region around $\sin^2(\beta - \alpha) \simeq \cos^2(\beta - \alpha)$ at low $\tan\beta$ where m_h and m_H are separated by more than $\simeq 10$ GeV [29, 18].

In Fig. 2(b), the corresponding discovery reach with the CMS experiment is shown. The complementarity of the colliders is clear. The LHC experiments are most

sensitive to large m_A , where m_h approaches its upper bound for the given choice of parameters. As m_A decreases, the $\phi b\bar{b}$ coupling increases, so that $B(\phi \rightarrow \gamma\gamma)$ and R' and R'' decrease. At the Tevatron, the region of large m_A and large $\tan\beta$ is harder to cover, because the $\phi b\bar{b}$ coupling decreases towards the Standard Model value, yielding $R \simeq 1$. Simultaneously, the lightest CP-even Higgs boson mass approaches its upper bound, so that more integrated luminosity is needed to probe this region. It is worth noting the change in the shape of the LHC contours between low and high luminosity, when the $gg \rightarrow \phi$ process becomes less important than the $t\bar{t}\phi/W\phi$ process. After the low luminosity run at the LHC (30 fb^{-1}), if the Tevatron obtains only 10 fb^{-1} of data, there remains a region uncovered by both colliders for $m_A \simeq 250 - 300 \text{ GeV}$ (there would also still be the hole at $\sin^2(\beta - \alpha) \simeq \cos^2(\beta - \alpha)$). The high luminosity run (but only with 100 fb^{-1}) is necessary to guarantee full coverage in this region, unless the Tevatron collects 20 fb^{-1} or more of integrated luminosity per experiment.

4.2 $\phi b\bar{b}$ suppression for large M_S

Figure 3 was generated using the choice of MSSM parameters $A_t = -\mu = 1.5 \text{ TeV}$ and $M_S = 1 \text{ TeV}$, which yields a suppression of the Higgs boson coupling to $b\bar{b}$ (and $\tau^+\tau^-$) in a significant portion of the $m_A - \tan\beta$ plane for the same Higgs boson that couples strongly to W and Z bosons (ϕ_W). An approximate analytic formula that shows the necessary relations between parameters can be obtained by setting $\mathcal{M}_{12}^2 = 0$ in Eq. (3.6) and was presented in Ref. [18]. In Fig. 3(a), the vanishing of $\sin\alpha$ is seen when $h \equiv \phi_W$ (region which remains uncovered by the Tevatron, in the upper part of the Figure), whereas the vanishing of $\cos\alpha$ occurs when $H \equiv \phi_W$ (region which remains uncovered by the Tevatron, in the lower part of the Figure). As alluded to earlier, the vanishing of the $\phi_W b\bar{b}$ and $\phi_W \tau^+\tau^-$ couplings greatly enhances $\text{BR}(\phi \rightarrow \gamma\gamma)$, and CMS has little difficulty in covering the complementary regions in the low luminosity run, as shown in Fig. 3(b).

After combining both discovery reaches, a small region, for which $\sin^2(\beta - \alpha) \simeq \cos^2(\beta - \alpha)$ persists, however, uncovered by both colliders. For clarity, we wish to emphasize again that LHC will have other means of testing the region of parameters which remain uncovered in our analysis by means of the production of other Higgs bosons of the low energy effective theory [14]. However, in this region of parameters, none of these Higgs bosons will have SM-like couplings, and hence will not directly test the mechanism of electroweak symmetry breaking. In addition, one of the unambiguous predictions of weak-scale supersymmetry (the upper bound on the mass of the SM-like Higgs) will not be tested directly.

4.3 Bottom Yukawa corrections

So far, our analysis has neglected corrections to the fermion Yukawa couplings from loop corrections. To illustrate the potential importance of these effects, we must

specify other parameters of the MSSM which, in the next-to-leading-logarithmic approximation, do not affect the CP-even Higgs masses and mixing angles in a relevant way (apart from the effects arising from the redefinition of the b -Yukawa coupling, which we will discuss below). Care must be taken in choosing these parameters, since an additional enhancement of the b Yukawa coupling at large values of $\tan\beta$ can cause the theory to become non-perturbative. Therefore, we consider an example similar to the one presented in Fig. 3, taking $A_t = -\mu = 1$ TeV. This still illustrates the suppression of the $\phi b\bar{b}$ coupling, but in a smaller region of the $M_A - \tan\beta$ plane. For this same choice of parameters, we then consider the effects of $\Delta(m_b)$ when the gluino mass parameter $M_{\tilde{g}}$ takes the values ± 5 TeV. From Eq. (3.12), we observe that the top quark-Yukawa coupling induced-contribution is negative for $A_t\mu < 0$, while a positive (negative) gluino mass will decrease (increase) $\Delta(m_b)$. The case of an overall positive correction (negative gluino mass) is illustrated in Fig. 4. The effect of the correction is minimal, since $\Delta(m_b)$ is never larger than about 0.3 at large $\tan\beta$. For the case of a negative correction, however, as seen in Fig. 5, the suppression of the $\phi b\bar{b}$ coupling for $m_A \gtrsim 130$ GeV is shifted to lower values of $\tan\beta$. Note that the suppression is now occurring because $\tan\alpha \simeq \Delta(m_b)/\tan\beta$, and *not* because the tree-level coupling vanishes $\sin\alpha \cos\alpha/\cos\beta \rightarrow 0$. According to Eq. (3.15), in the regions of parameter space where the tree-level $\phi b\bar{b}$ vanishes, the $\phi b\bar{b}$ coupling can be substantial and the $\phi\tau^+\tau^-$ coupling is suppressed. When the $\phi b\bar{b}$ coupling suppression occurs, the $\phi\tau^+\tau^-$ coupling will typically not vanish, as demonstrated in Eq. (3.17).

There are several phenomenological consequences of the mismatch in the behavior of the $\phi b\bar{b}$ and $\phi\tau^+\tau^-$ couplings. First, in the previous examples, we observed that the $\phi_W \rightarrow b\bar{b}$ channel at the Tevatron (or the LHC) can cover those regions where the $\phi_W \rightarrow \gamma\gamma$ channel is suppressed. Secondly, in such examples, the simultaneous vanishing of the $\phi b\bar{b}$ and the $\phi\tau^+\tau^-$ couplings led to an enhancement of $\text{BR}(\phi \rightarrow \gamma\gamma)$. However, the enhancement in the region where $\phi b\bar{b}$ is suppressed will generally not be as large as naively expected, since $\Gamma(\phi \rightarrow \tau^+\tau^-)$ can still be substantial. Still, the complementarity of the Tevatron and the LHC experiments in the search for the Higgs ϕ_W remains clear. Given the fact that the decay $\phi_W \rightarrow \tau^+\tau^-$ may be dominant in this region, it is important to consider $\phi_W \rightarrow \tau^+\tau^-$ signatures at the Tevatron and LHC. Preliminary results in this direction have been presented in Ref. [12].

An illustration of the possible variation of the $\phi_W \rightarrow b\bar{b}$ and $\phi_W \rightarrow \tau^+\tau^-$ decay modes in parameter space is presented in Fig. 6, which shows the function R of Eq. (3.4) for the $b\bar{b}$ final state (R_b) (a) and the $\tau^+\tau^-$ final state (R_τ) (b) for the same parameters as in Fig. 5. Note the large region where R_b is greater than the SM value, where as R_τ is below it. Of course, there is a compensating region along contours of $\tan\alpha \simeq \Delta(m_b)/\tan\beta$ at very large $\tan\beta$ where $\phi_W \rightarrow \tau^+\tau^-$ is the dominant decay mode. In terms of area covered in the $M_A - \tan\beta$ plane, the former is more significant than the latter. It is also worth noting that both R values approach their

SM values in the limit of large M_A . Indeed, when M_A is large *and* M_S is large, the effect of the radiative corrections vanish. When M_A is fixed and M_S is arbitrarily large, however, the radiative corrections will in general be relevant [18], a reflection of the lack of supersymmetry in the low energy effective theory.

It is important to emphasize that the nice complementarity between the $\phi_W \rightarrow b\bar{b}$ and $\phi_W \rightarrow \gamma\gamma$ decay channels holds due to the fact that the former is, in general, the dominant Higgs decay channel. This complementarity does not extend to the $\phi_W \rightarrow \tau^+\tau^-$ channel. Indeed, in the above example, we see region of parameters for which $\phi_W \rightarrow \tau^+\tau^-$ is suppressed and, due to a slight enhancement of $\phi \rightarrow b\bar{b}$ decay rate in the same region of parameters, the LHC reach in the $\phi_W \rightarrow \gamma\gamma$ channel is also suppressed.

4.4 Cancellations from the sbottom sector

In the previous examples, we showed how relatively large values of $A_t \simeq -\mu$ led to the suppression of the $\phi b\bar{b}$ coupling in the large $\tan\beta$ regime. We demonstrate that this can also occur when $A_b \simeq \mu$ in Figs. 7, and 8. The effect of A_b , however, is in general much weaker than the A_t one, and becomes only relevant for large values of the bottom Yukawa coupling, that is for values of $\tan\beta \simeq m_t/m_b$. To show this, in these figures, we choose moderate values of A_b and μ , taking $A_t = 0$. The vanishing of A_t leads, in general, to masses that are of the order of the ones obtained in the minimal mixing case, although they can be further reduced, due to the μ -induced terms discussed above, for large values of $\tan\beta$. Also, the top Yukawa contribution to $\Delta(m_b)$ vanishes for $A_t = 0$. In Fig. 7, we have chosen $A_b = \mu = 1.25$ TeV and $M_{\tilde{g}} = .5$ TeV, leading to $\Delta(m_b) > 0$. No relevant modification in the reach is found compared to the minimal mixing case (Fig. 2). Indeed, for the parameters chosen, the suppression of the $\phi b\bar{b}$ coupling takes place at values of $\tan\beta$ larger than the ones considered in this analysis. To observe the suppression for positive corrections, we would need to choose larger values of A_b and μ .

For $M_{\tilde{g}} = -.5$ TeV, which yields $\Delta(m_b) < 0$, we observe the suppression of the $\phi b\bar{b}$ coupling in Fig. 8, in region of parameter space in which $\tan\alpha \simeq \Delta(m_b)/\tan\beta$. This leads to holes in the regions of parameter space to be tested at LEP and the Tevatron in the $\phi_W \rightarrow b\bar{b}$ channel, but a compensating increase in $\phi_W \rightarrow \gamma\gamma$ rate in the same regions of parameters. Since we have also included the bottom Yukawa coupling corrections to the calculation of the mass spectrum, we observe the reappearance of the LEP exclusion at large $\tan\beta$, due to a reduction of the Higgs boson mass.

Although the above provides only an extreme example for which only the A_b -induced effects were considered, it shows in a clear way the relative importance of the effects on the Higgs mass matrix elements induced by the presence of non-trivial mixing in the sbottom and stop sectors. In the following sections, we shall present examples in which $A_t \simeq A_b \neq 0$.

4.5 Light stop and large mixing

In the minimal mixing model investigated in section 4.1, the SUSY scale M_S was set to 1 TeV, but the mixing term \tilde{A}_t was zero. In the present case, we consider equal values for the left- and right-handed soft supersymmetry-breaking squark masses of the third generation, and adjust the common value to yield a lightest top squark mass of 200 GeV. This is meant to demonstrate the possibility of large corrections to the ϕgg and $\phi\gamma\gamma$ couplings from light sparticles. In addition, this lowers the scale M_S . We fix $\mu = -0.3$ TeV, and $A_t = 1$ TeV, so that stop mixing is large ⁶. This is motivated by the form of the $\{h, H\}\tilde{t}\tilde{t}$ coupling (written here in the interaction basis):

$$\begin{aligned} \frac{2m_t^2}{v \sin \beta} \{\cos \alpha, \sin \alpha\} - \frac{2M_Z^2}{v} \{\sin(\alpha + \beta), -\cos(\alpha + \beta)\} (1/2 - 2/3 \sin^2 \theta_W) & \quad (LL) \\ \frac{2m_t^2}{v \sin \beta} \{\cos \alpha, \sin \alpha\} - \frac{2M_Z^2}{v} \{\sin(\alpha + \beta), -\cos(\alpha + \beta)\} 2/3 \sin^2 \theta_W & \quad (RR) \\ \frac{m_t}{v \sin \beta} [A_t \{\cos \alpha, \sin \alpha\} + \mu \{\sin \alpha, -\cos \alpha\}] & \quad (LR) \end{aligned}$$

where we have denoted the components in parentheses. For large LR mixing, the terms proportional to A_t and μ can dominate the stop-Higgs couplings. For a Higgs with SM-like couplings to the gauge bosons, in the moderate and large $\tan \beta$ regime, A_t is the relevant mixing parameter determining the strength of this coupling. For large values of m_A and arbitrary values of $\tan \beta$, this coupling is proportional to \tilde{A}_t , which is approximately equal to A_t in the large $\tan \beta$ regime.

In this region of parameters, the Tevatron can discover a Higgs ϕ_W in most of the parameter space with about 20 fb^{-1} . One observes from Fig. 9(a) that although the stops are lighter in this case, the reach at the Tevatron is somewhat suppressed with respect to the minimal mixing case, and 30 fb^{-1} are necessary to cover the whole parameter space, with the exception of the region of parameters for which $\sin^2(\beta - \alpha) \simeq \cos^2(\beta - \alpha)$. The origin of the relative suppression in the discovery reach is the upper bound on the lightest CP-even Higgs mass, which increases substantially when $\tilde{A}_t \neq 0$. For instance, while for the minimal mixing case this upper bound is below 115 GeV, values close to 120 GeV are obtained in the case under analysis.

As noted earlier, light top and bottom squarks can have a large effect on the one-loop suppressed partial widths $\Gamma(\phi \rightarrow gg)$ and $\Gamma(\phi \rightarrow \gamma\gamma)$. The relation between these two quantities is reciprocal, and depends on the size of A_t and μ . When the stop mixing mass parameters (in particular A_t) become large, the width $\Gamma(\phi \rightarrow gg)$ can be greatly decreased since the light top squark loop contribution can partially or

⁶As has been observed in Ref. [26], precision electroweak measurements tend to disfavor the presence of light third generation squarks with large mixing angles. Most of the parameters considered in this subsection, as in the following two, are only marginally consistent with the precision electroweak data.

totally cancel the top quark loop induced one. In Fig. 9(b), it is clear that R' , Eq. (3.18) is widely suppressed, and this is reflected in the fact that the low luminosity run of the LHC cannot observe the Higgs boson that couples strongly to the W and Z boson in the gluon fusion channel. In the high luminosity run, the dependence on $\Gamma(\phi \rightarrow gg)$ is weakened, and the reach is dominated by the $t\bar{t}\phi/W\phi$ channels (see also [13]). In this Higgs mass range, the LHC sensitivity in these channels depends only weakly on the Higgs mass and for high luminosity the LHC discovery reach becomes similar to the one in the minimal mixing case.

The complementarity of the Tevatron and LHC colliders in this case is similar to the case of minimal mixing, although somewhat larger luminosities in both colliders are needed in order to obtain full coverage of the MSSM parameter space.

4.6 $\phi b\bar{b}$ coupling suppression for light stops

Since we have identified two interesting effects, namely the suppression of the $\phi b\bar{b}$ coupling from Higgs mixing and the suppression of one-loop couplings from large stop mixing, one may wonder if both can occur. The conditions for the cancellation of \mathcal{M}_{12}^2 , and hence for $\phi b\bar{b}$ suppression, can be determined analogously to the large M_S case, but since the stop mixing effects become larger, the approximate formulae Eq. (3.6) is no longer valid, and one should work with the full effective potential computation [6]. One example occurs for $\mu = 1$ TeV, $A_t = .65$ TeV, and a lightest stop mass fixed at 200 GeV as before. We display an example in Figure 10. Since the stop mixing effects we are considering are larger than in the previous cases, the cancellation of the $\phi b\bar{b}$ coupling occurs for larger values of the CP-odd Higgs mass. Indeed, Fig. 10(a) reveals that the region of $\phi b\bar{b}$ suppression is shifted substantially.

Most interesting is the fact that LEP could discover a Higgs boson with strong couplings to W and Z bosons at large $\tan\beta$. As noticed before, this is just a reflection of the suppression of the Higgs mass induced by the μ parameter at large values of $\tan\beta$, as shown in the expression of \mathcal{M}_{22}^2 in Eq. (3.6). Of course, in the regions of $\phi b\bar{b}$ suppression, neither LEP nor the Tevatron have any reach (we are not considering a possible enhancement of the tau lepton coupling, which, as explained before, can take place if $\Delta(m_b) \neq \Delta(m_\tau)$).

Because of the suppression of the $\phi b\bar{b}$ coupling, the LHC, Fig. 10(b), has significant reach in the regions complementary to LEP and the Tevatron. Observe that the reach at low $\tan\beta$ and large $m_A \gtrsim 350$ GeV is slightly less than for the minimal mixing model, because of a small increase of the $\phi b\bar{b}$ coupling. However, for the same value of $\tan\beta$ and m_A , the lightest CP-even Higgs mass increases, and therefore the increase of the $\text{BR}(h \rightarrow b\bar{b})$ is not reflected in an increase of the Tevatron reach.

More important, there are region of parameters, at large values of $\tan\beta$, for which the Higgs becomes accessible to the three colliders with relatively small luminosity. This would provide a perfect situation: A Higgs with SM-like couplings to the gauge

bosons will be discovered at LEP by the end of the year 2000, and its properties will be further tested at the Tevatron and LHC colliders.

4.7 $\phi b\bar{b}$ coupling enhancement and light third generation squarks.

A large value of $\tilde{A}_b \equiv A_b - \mu \tan \beta$ can have significant consequences when the bottom squark is also light. In Fig. 11(b), one observes a general suppression of R' and R'' throughout most of the $M_A - \tan \beta$ plane. For this example, we have set $A_t = A_b = -0.5$ TeV, $\mu = -1$ TeV, and all third generation squark parameters equal and tuned to yield a bottom squark mass of 200 GeV. For small values of the ratio of Higgs vacuum expectation values ($\tan \beta < 2$) this choice of parameters may lead to too light top squarks, with masses below the present experimental bound, or even negative ones. In these cases, we have increase the squark masses by setting a lower bound on the lightest bottom squark of about 300 GeV. Although this implies a slight discontinuity of the parameters chosen to perform the figures, this does not affect the physical results since for such light stops and sbottoms the $\tan \beta < 2$ regime is already ruled out by LEP2 data.

Since \tilde{A}_t and \tilde{A}_b are large, and the bottom and top squarks are light, one might expect that $\Gamma(\phi \rightarrow gg)$ will decrease and $\Gamma(\phi \rightarrow \gamma\gamma)$ will increase. This is true, but any further expectation that $\text{BR}(\phi \rightarrow \gamma\gamma)$ increases is nullified by the fact that, for this choice of parameters, the bottom quark coupling to the Higgs ϕ_W is enhanced with respect to the Standard Model expectation, inducing a decrease of the $\text{BR}(\phi_W \rightarrow \gamma\gamma)$. Had we chosen the opposite sign of μ , an increase of the $\text{BR}(\phi_W \rightarrow \gamma\gamma)$ with respect to the SM value would have been observed, as in the previous section.

Because of the enhancement of $\text{BR}(\phi \rightarrow b\bar{b})$ and given that the Higgs ϕ_W mass is below 112 GeV (it becomes smaller at small and large values of $\tan \beta$), it is particularly easy to probe this region of the MSSM parameters. For instance, LEP can probe a significant portion of the $M_A - \tan \beta$ plane (LEP will be sensitive to the region connected by the narrow strip around $M_A \simeq 135$ GeV) as seen in Fig. 11(a), and the Tevatron would only need a substantial luminosity upgrade to cover the difficult region near $M_A \simeq 120$ GeV.

5. Conclusions

To test if the mechanism of electroweak symmetry breaking is indeed generated by a fundamental scalar, as postulated in the minimal Standard Model and its supersymmetric extension, it will be necessary to observe the Higgs boson which is responsible for the W and Z boson masses, and hence, has SM-like couplings to these gauge bosons. Otherwise, it will be difficult to conclude if the mechanism of electroweak symmetry breaking relies on a weakly or strongly coupled model, or, if the low energy Higgs sector fulfills the properties demanded in the MSSM, for instance the

upper bound on the lightest CP-even Higgs mass. In theories with more than one Higgs doublet, the real part of the neutral Higgs combination which acquires vacuum expectation value is not necessarily associated with a physical mass eigenstate. However, there are large regions of the MSSM parameter space where one of the CP-even Higgs bosons couples in a Standard Model way to the W and Z bosons and up quarks and, hence, can be identified as the dominant source of electroweak symmetry breaking. We have denoted such a Higgs boson as ϕ_W . Interestingly enough, the ϕ_W couplings to bottom quarks and τ -leptons, which control the dominant decay modes of the Standard Model Higgs, can be highly non-standard. Therefore, the full experimental program to discover the Higgs ϕ_W must account for the possibility that some of its standard signatures may be significantly modified. A suppression of the standard signatures may occur for natural choices of the soft supersymmetry-breaking parameters of the low-energy effective theory. When viewed in this light, one sees that measurements at LEP and Tevatron can provide important information about the Higgs sector which will be complemented by measurements at the LHC. On the other hand, in the regions of parameter space where the Higgs searches at the LEP and Tevatron colliders become difficult, the LHC will, in general, be able to find the Higgs ϕ_W at relatively low integrated luminosities, $\mathcal{L} < 100 \text{ fb}^{-1}$. We have presented several explicit choices of MSSM parameters which demonstrate this point, including the possibility that the top and bottom squarks are relatively heavy or light.

In general, we have observed some patterns in the choices of soft supersymmetry-breaking parameters that lead to difficulties at either LEP/Tevatron or LHC, but give a complementary enhanced signature at the other collider(s):

- When $A_t\mu < 0$ or $A_b\mu > 0$, with parameter values of the order of the scale $M_S \simeq 1 \text{ TeV}$, there can be a suppression of the $\phi_W b\bar{b}$ coupling, which limits the $\phi_W \rightarrow b\bar{b}$ channel at LEP/Tevatron. Complementary to this, $\text{BR}(\phi_W \rightarrow \gamma\gamma)$ is enhanced at the LHC. Hence, while for these conditions the discovery of the Higgs ϕ_W at LEP and the Tevatron will require very high luminosities, even a low luminosity run at the LHC will be sufficient to discover the Higgs ϕ_W .
- As the values of A_t, A_b and μ are lowered, the $\phi_W b\bar{b}$ coupling can still be suppressed in the presence of large radiative corrections to the $\phi_W b\bar{b}$ coupling, $\Delta(m_b)$, which are proportional to $\tan\beta$ and can be of order one for large $\tan\beta$. In this case, the suppression occurs because the relation $\tan\alpha \simeq \Delta(m_b)/\tan\beta$ holds. There is also a mismatch between the $\phi_W b\bar{b}$ and $\phi_W \tau^+\tau^-$ couplings, to be discussed below. As before, the complementarity arises because the LHC reach in the $\phi_W \rightarrow \gamma\gamma$ channel increases (decreases) when the bottom Yukawa coupling is decreased (increased).
- If M_S is decreased, but the other parameters still obtain values near 1 TeV, then

the $\phi_W b\bar{b}$ suppression occurs for smaller values of $\tan\beta$ and at large values of m_A . At large $\tan\beta$, the mass of the Higgs ϕ_W decreases from its upper bound, which is achieved at intermediate values of $\tan\beta$ between 10 and 20, and LEP becomes sensitive to the Higgs ϕ_W , but not in the regions where the Tevatron reach is also suppressed. The signal rate in the $\phi_W \rightarrow \gamma\gamma$ channel is again enhanced in those regions inaccessible at the LEP/Tevatron.

- A small top squark mass, a large value for A_t and moderate μ can decrease $\Gamma(\phi_W \rightarrow gg)$ through the interference of top and top squark loops, which limits the channel $gg \rightarrow \phi_W \rightarrow \gamma\gamma$ at the LHC. Simultaneously, the $\phi_W b\bar{b}$ coupling can be enhanced or suppressed over the SM value, because of the contribution of A_t and μ to the mixing in the Higgs sector. If the $\phi_W b\bar{b}$ coupling is enhanced, the $\text{BR}(\phi_W \rightarrow \gamma\gamma)$ can actually also decrease. Because of the increase in $\text{BR}(\phi_W \rightarrow b\bar{b})$, the channel $\phi_W \rightarrow b\bar{b}$ at the Tevatron can be used to cover the problematic regions at the LHC, provided that the experiments at the Tevatron receive enough luminosity. On the other hand, if the $\phi_W b\bar{b}$ coupling is suppressed, there will be a further increase in $\text{BR}(\phi_W \rightarrow \gamma\gamma)$ which enhances the reach of the LHC in the $t\bar{t}\phi_W$ and $W\phi_W$ channels.
- Large values for A_b, A_t and μ with light bottom and top squarks may lead to a wide suppression of $\text{BR}(\phi_W \rightarrow \gamma\gamma)$, because the $\phi_W b\bar{b}$ coupling can be significantly enhanced. This limits all of the $\phi_W \rightarrow \gamma\gamma$ channels at the LHC. The upper bound on the Higgs boson mass is reduced in conjunction with the increase in $\text{BR}(\phi_W \rightarrow b\bar{b})$, so that LEP and the Tevatron cover most of the complementary regions of the $M_A - \tan\beta$ plane. High luminosity is only required at the Tevatron to cover the regions where neither CP-even Higgs boson has SM-like couplings to the gauge bosons, $\sin^2(\beta - \alpha) \simeq \cos^2(\beta - \alpha)$.
- For MSSM parameter choices where the Higgs mixing would cause a suppression of both the $\phi_W b\bar{b}$ and $\phi_W \tau^+ \tau^-$ couplings at tree-level, large radiative corrections from SUSY-breaking effects can modify the bottom and tau decay rates in different ways. As a result, one may observe $\phi_W(\rightarrow b\bar{b})$ without $\phi_W(\rightarrow \tau^+ \tau^-)$. In the regions where there is a suppression of the $\phi_W \tau^+ \tau^-$ coupling, there is not necessarily an enhancement of $\text{BR}(\phi_W \rightarrow \gamma\gamma)$, because the $\phi_W b\bar{b}$ coupling can be of the order of the Standard Model value. In the presence of large SUSY-breaking effects, the suppression of the $\phi_W b\bar{b}$ coupling occurs when $\tan\alpha \simeq \Delta(m_b)/\tan\beta$. For this value of $\tan\alpha$, the $\phi_W \tau^+ \tau^-$ coupling will not vanish, in general, and $\phi_W \rightarrow \tau^+ \tau^-$ may be the dominant decay.

While our analysis has emphasized the complementarity of LEP and the Tevatron in the $\phi_W(\rightarrow b\bar{b})$ channels to the LHC in the $\phi_W(\rightarrow \gamma\gamma)$ channels, our results are more general. If the experiments at the Tevatron do not receive enough luminosity, then

the $t\bar{t}\phi_W(\rightarrow b\bar{b})$ channel, which to a good approximation has the same parameter dependence as the $W\phi_W(\rightarrow b\bar{b})$ channel, at the LHC will be complementary to the $\phi_W(\rightarrow \gamma\gamma)$ channels (the $WW \rightarrow \phi_W(\rightarrow \tau^+\tau^-)$ channel may also be useful). On the other hand, with enough luminosity, the Tevatron may be able to observe the $\phi_W(\rightarrow \gamma\gamma)$ channel when the $\phi_W b\bar{b}$ coupling is greatly suppressed. Regardless which of these scenarios is realized, the next generation of measurements at LEP, the Tevatron and the LHC can most likely reveal the nature of electroweak symmetry breaking by observing or excluding a light Higgs boson with Standard Model-like couplings to the W and Z bosons.

Acknowledgements We thank D. Denegri and E. Richter-Was for providing information about various channels. We would also like to thank G. Azuelos, J. Gunion, H. Haber and J. Womersley for interesting discussions. M.C. and C.W. would like to thank the Aspen Center for Physics, where part of this work has been done. Work supported in part by the U.S. Department of Energy, High Energy Physics Division, under Contract W-31-109-Eng-38.

A. Relations between the CP even Higgs masses

To derive Eq. (1.2), we start with the Higgs squared-mass matrix elements parametrized in the following form (see Eq. (3.6)),

$$\begin{aligned}\mathcal{M}_{11}^2 &= m_A^2 \sin^2 \beta + \Delta_{11} \\ \mathcal{M}_{22}^2 &= m_A^2 \cos^2 \beta + \Delta_{22} \\ \mathcal{M}_{12}^2 &= -m_A^2 \cos \beta \sin \beta + \Delta_{12},\end{aligned}\tag{A.1}$$

where Δ_{ij} denotes terms independent of m_A^2 . For very large values of m_A^2 , the heaviest CP-even Higgs mass $m_H^2 \simeq m_A^2$ and the determinant of the Higgs squared mass matrix will be equal to $m_A^2 \times m_h^2|_{m_A^2 \gg M_Z^2}$, where the last term is the upper bound on the lightest CP-even Higgs mass. This upper bound can be obtained by taking the terms proportional to m_A^2 in the determinant of the Higgs squared-mass matrix,

$$\begin{aligned}m_h^2|_{m_A^2 \gg M_Z^2} &\simeq \Delta_{11} \cos^2 \beta + \Delta_{22} \sin^2 \beta + 2\Delta_{12} \cos \beta \sin \beta \\ &= \mathcal{M}_{11}^2 \cos^2 \beta + \mathcal{M}_{22}^2 \sin^2 \beta + 2\mathcal{M}_{12}^2 \cos \beta \sin \beta\end{aligned}\tag{A.2}$$

Since the mass matrix is diagonalized by a rotation with mixing angle α , we have

$$\begin{aligned}\mathcal{M}_{11}^2 &= m_h^2 \sin^2 \alpha + m_H^2 \cos^2 \alpha \\ \mathcal{M}_{22}^2 &= m_h^2 \cos^2 \alpha + m_H^2 \sin^2 \alpha \\ \mathcal{M}_{12}^2 &= (m_H^2 - m_h^2) \sin \alpha \cos \alpha.\end{aligned}\tag{A.3}$$

Substituting Eq. (A.3) into Eq. (A.2) yields the desired relation, namely,

$$m_h^2|_{m_A^2 \gg M_Z^2} = m_h^2 \sin^2(\beta - \alpha) + m_H^2 \cos^2(\beta - \alpha).\tag{A.4}$$

Let us emphasize that, in the above, we have ignored the small differences between pole masses and running masses, while we have defined all matrix elements at the scale m_t , ignoring the effects of the decoupling of the heavy Higgs doublet. These effects, however, are only relevant for $m_A \gg M_Z$, in which case $\sin^2(\beta - \alpha) \rightarrow 1$ independently of the scale of definition. It is easy to prove that $\cos^2(\beta - \alpha) = \mathcal{O}(M_Z^4/m_A^4)$ for the same conditions, and therefore the above equality, Eq. (A.4), is satisfied in a straightforward way.

References

- [1] The LEP Electroweak Working Group, and the SLD Heavy Flavor and Electroweak Groups: D. Abbaneo *et al.*, Internal Note CERN-EP/99-15; J. Erler, hep-ph/99042235, and references therein.
- [2] M. Carena, P. Zerwas, and the Higgs Physics Working Group, *Physics at LEP2, Vol. 1*, edited by G. Altarelli, T. Sjöstrand, and F. Zwirner, CERN Report No. 96-01.
- [3] M. Felcini, Higgs searches at LEP, talk presented at the Moriond Conference, Electroweak Session, March 1999.
- [4] R. Hempfling and A. Hoang, *Phys. Lett.* **331B** (1994) 99; J. Kodaira, Y. Yasui and K. Sasaki, *Phys. Rev.* **D50** (1994) 7035.
- [5] J. Casas, J.R. Espinosa, M. Quiros and A. Riotto, *Nucl. Phys.* **B436** (1995) 3.
- [6] M. Carena, J.-R. Espinosa, M. Quiros and C.E.M. Wagner, *Phys. Lett.* **355B** (1995) 209; M. Carena, M. Quiros and C.E.M. Wagner, *Nucl. Phys.* **B461** (1996) 407.
- [7] H. Haber, R. Hempfling and A.H. Hoang, *Z. Phys.* **C57** (1997) 539.
- [8] S. Heinemeyer, W. Hollik and G. Weiglein, *Phys. Rev.* **D58** (1998) 091701; *Eur. Phys. J.* **C9** (1999) 343.
- [9] See, for example, P. Chankowski and S. Pokorski, hep-ph/9707497, in *Perspectives in Supersymmetry*, ed. by G. Kane, World Scientific, 1997; M. Carena, D. Choudhury, S. Raychaudhuri and C.E.M. Wagner, *Phys. Lett.* **B414** (1997) 414.
- [10] M. Carena, P. Chankowski, S. Pokorski and C.E.M. Wagner, *Phys. Lett.* **B 441** (1998) 205.
- [11] M. Carena, J. Conway, H. Haber, J. Hobbs *et. al.*, Report of the Higgs Working Group of the RunII Workshop, Fermilab, 1999, to appear. Results available at <http://fnth37.fnal.gov/higgs.html>
- [12] D. Rainwater and D. Zeppenfeld, *JHEP* **12** (1997) 005; D. Rainwater, D. Zeppenfeld and K. Hagiwara, *Phys. Rev.* **D59** (1999) 014037; T. Plehn, D. Rainwater and D. Zeppenfeld, *Phys. Lett.* **B454** (1999) 297.

- [13] G. Belanger, F. Boudjema and K. Sridhar, hep-ph/9904348; A. Dedes and S. Moretti, hep-ph/9904491.
- [14] E. Richter–Was, D. Froidevaux, F. Gianotti, L. Poggioli, D. Cavalli, and S. Resconi, *Int. Jour. Mod. Phys.* **13** (1998) 1371.
- [15] G. Acquistapace *et al.* [CMS Collaboration], CERN-LHCC-97-10; R. Kinnunen and D. Denegri, CMS-NOTE-1997-057; K. Lassila–Perini, CMS-THESIS-1998-147.
- [16] M. Carena, J. Ellis, S. Lola and C.E.M. Wagner, preprint CERN-TH/99-173, hep-ph/9906362.
- [17] J.A. Coarasa, R.A. Jimenez, and J. Sola, *Phys. Lett.* **B389** (1996) 312; R.A. Jimenez and J. Sola, *Phys. Lett.* **B389** (1996) 53.
- [18] M. Carena, S. Mrenna and C.E.M. Wagner, hep-ph/9808312; to be published in *Phys. Rev. D*.
- [19] A. Dabelstein, *Nucl. Phys.* **B456** (1995) 25.
- [20] See the transparencies from the talks of H. Logan, M.J. Herrero at SUSY99.
- [21] L. Hall, R. Rattazzi and U. Sarid, *Phys. Rev. D* **50** (1994) 7048; R. Hempfling *Phys. Rev. D* **49** (1994) 6168.
- [22] M. Carena, M. Olechowski, S. Pokorski and C.E.M. Wagner, *Nucl. Phys* **B426** (1994) 269.
- [23] D. Pierce, J. Bagger, K. Matchev, and R. Zhang, *Nucl. Phys.* **B491** (1997) 3.
- [24] For related work, see, F. Borzumati, G.R. Farrar, N. Polonsky and S. Thomas, hep-ph/9712428; preprint CERN-TH/98-383, hep-ph/9902443.
- [25] H. Baer and J.D. Wells, *Phys. Rev.* **D57** (1998) 4446; W. Loinaz and J.D. Wells, *Phys. Lett.* **B445** (1998) 178.
- [26] A. Djouadi, *Phys. Lett.* **B435** (1998) 101.
- [27] As presented by P. Janot (CERN) at the Chamonix-IX Workshop, January 28, 1999.
- [28] A. Djouadi, J. Kalinowski, and M. Spira, *Comput. Phys. Commun.* 108 (1998) 56.
- [29] H. Baer, B.W. Harris and X. Tata, *Phys. Rev.* **D59** (1999) 015003.

5 σ Higgs Discovery Contours

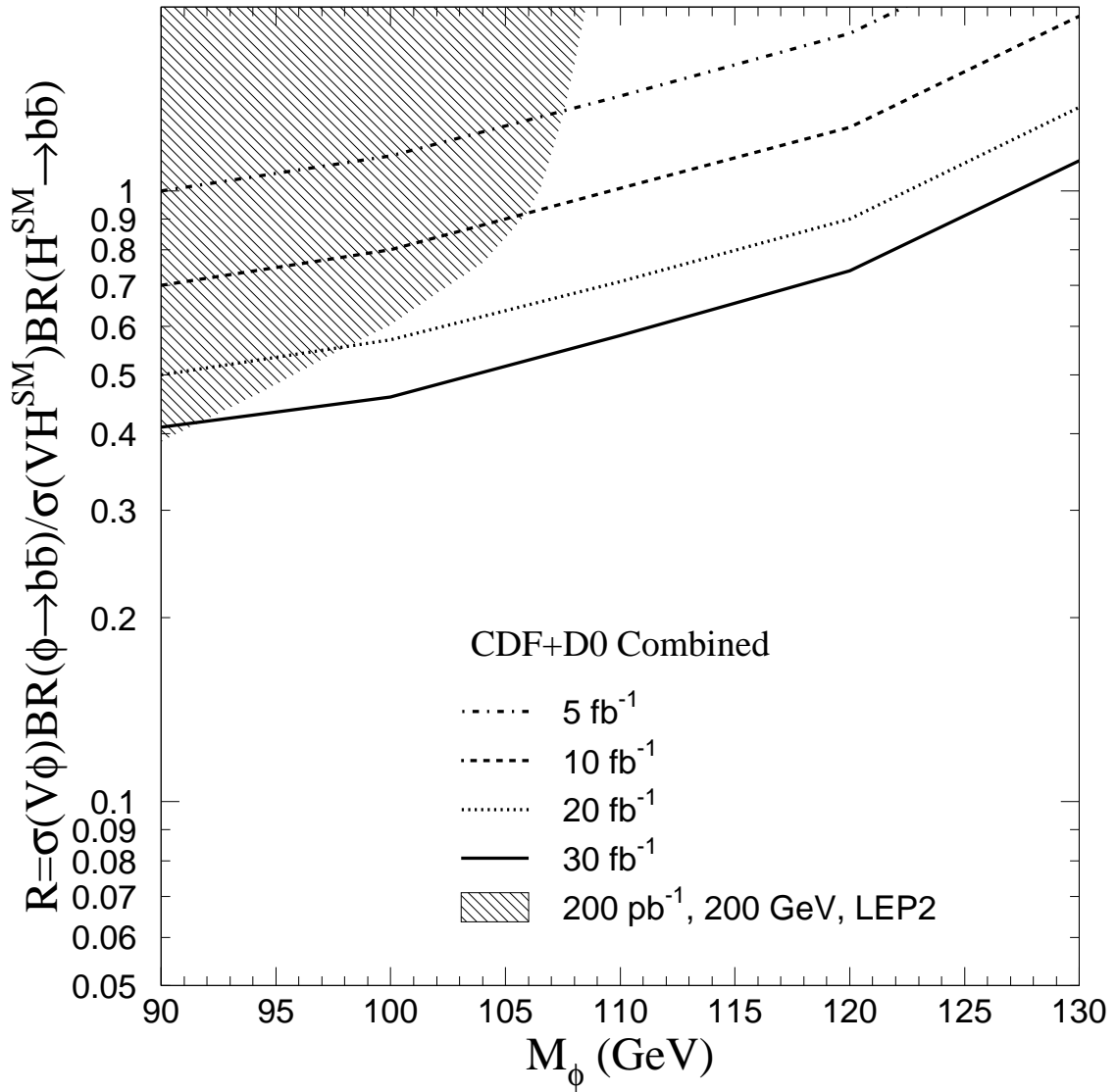


Figure 1: Sensitivity of the Standard Model Higgs searches at LEP and the Tevatron (for different total integrated luminosity).

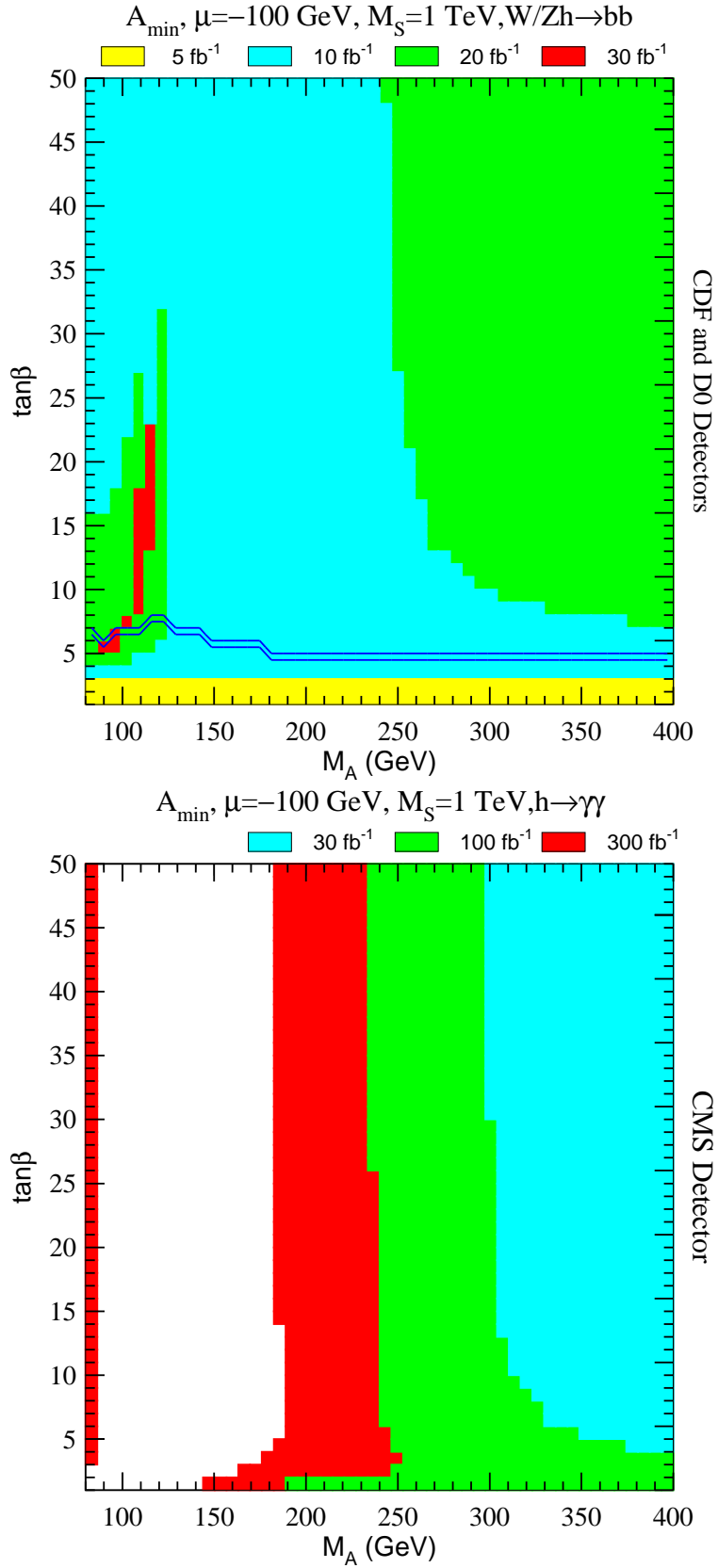


Figure 2: Discover reach of the LEP, Tevatron and LHC experiments in the minimal mixing model, as defined in the text.

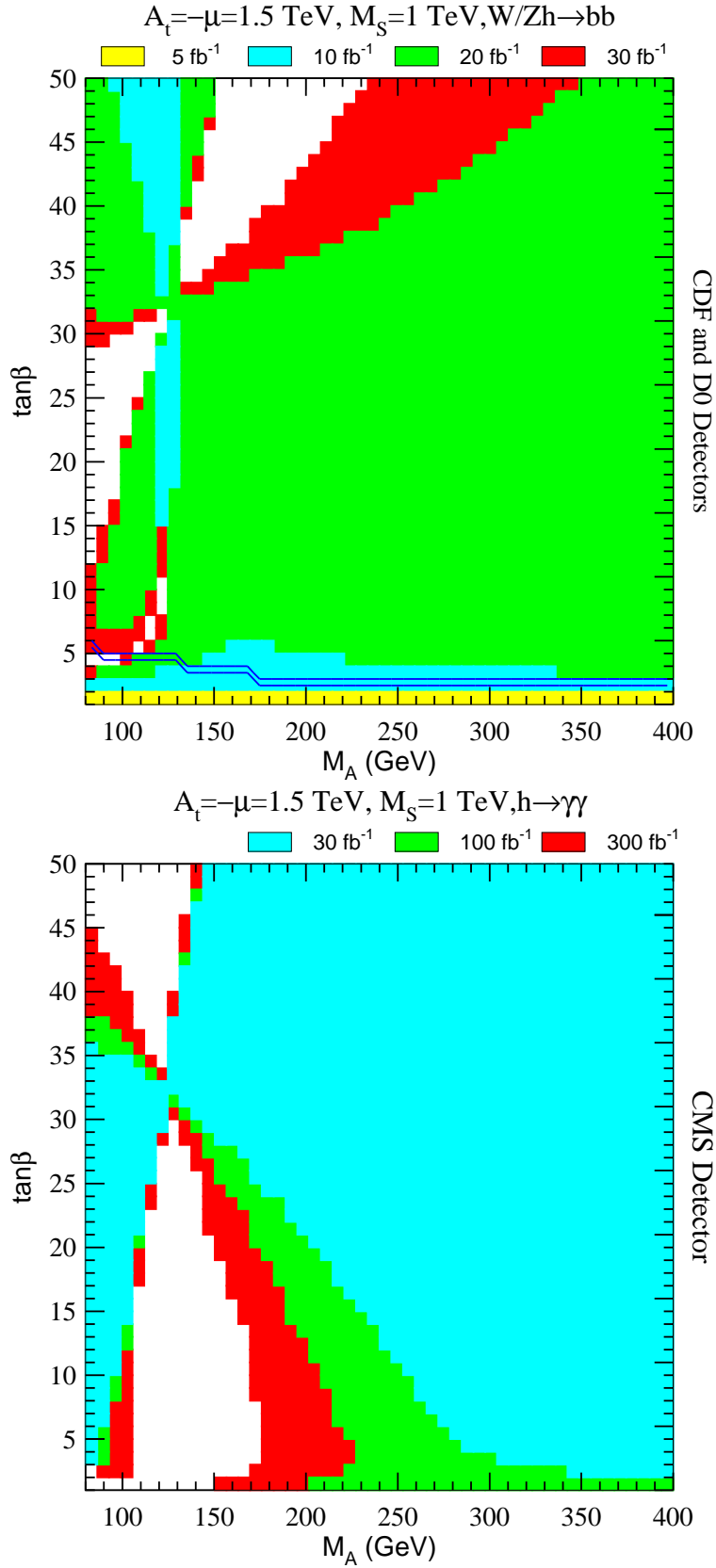


Figure 3: Same as Fig. 2 but for $A_t = -\mu = 1.5 \text{ TeV}, M_S = 1 \text{ TeV}$

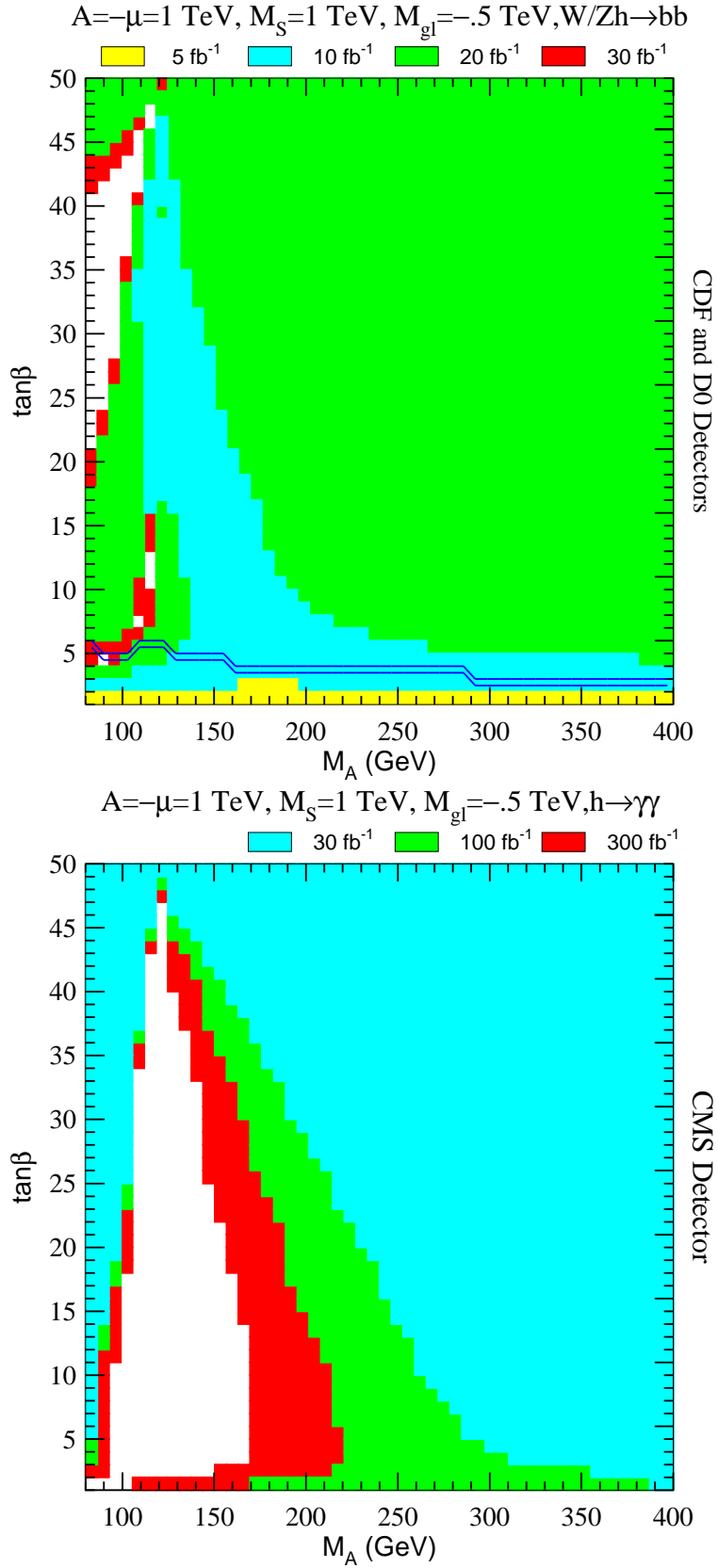


Figure 4: Same as Fig. 2, but for $A_t = -\mu = 1 \text{ TeV}$, and including the effects of the bottom mass corrections, $\Delta(m_b)$, calculated using $M_{\tilde{g}} = -0.5 \text{ TeV}$.

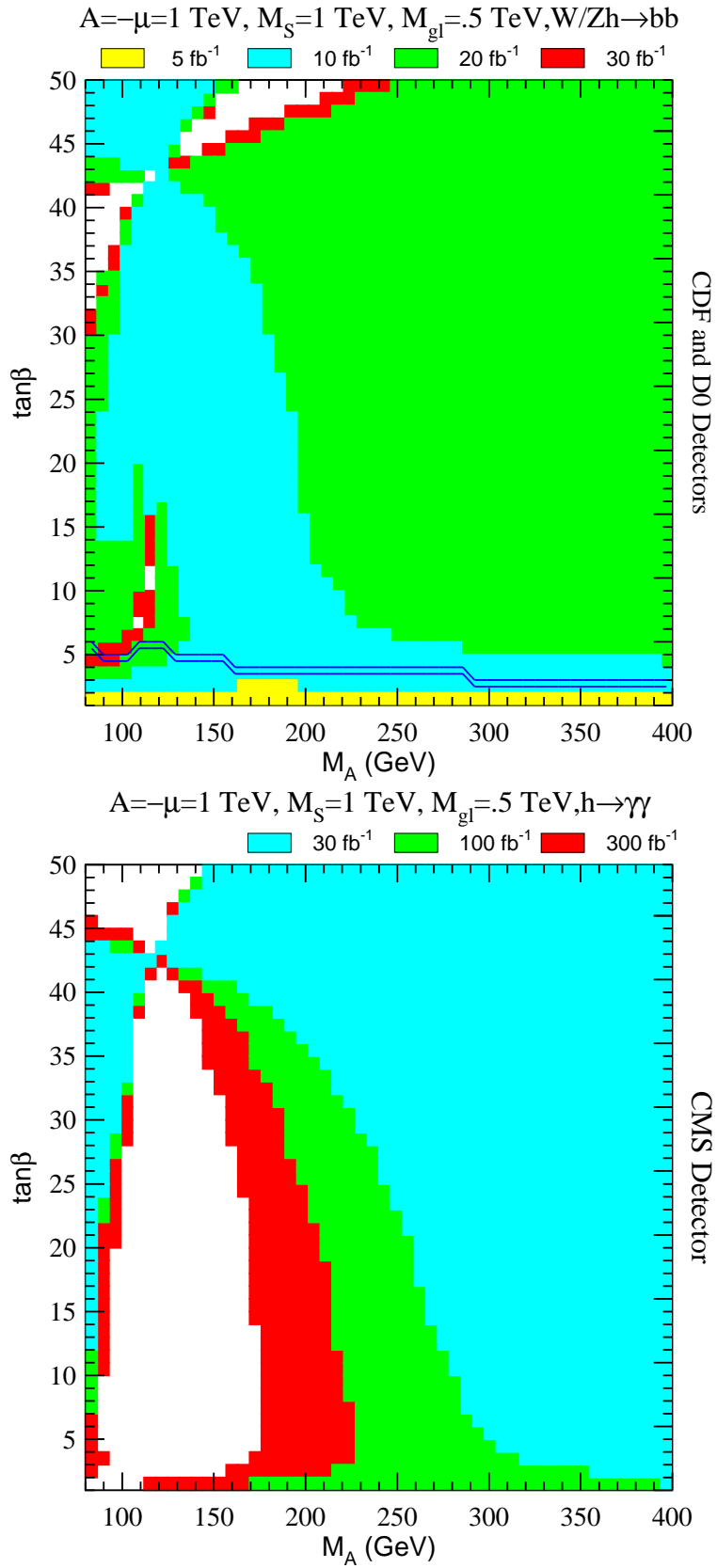


Figure 5: Same as Fig. 4, but for $M_{\tilde{g}} = .5 \text{ TeV}$.

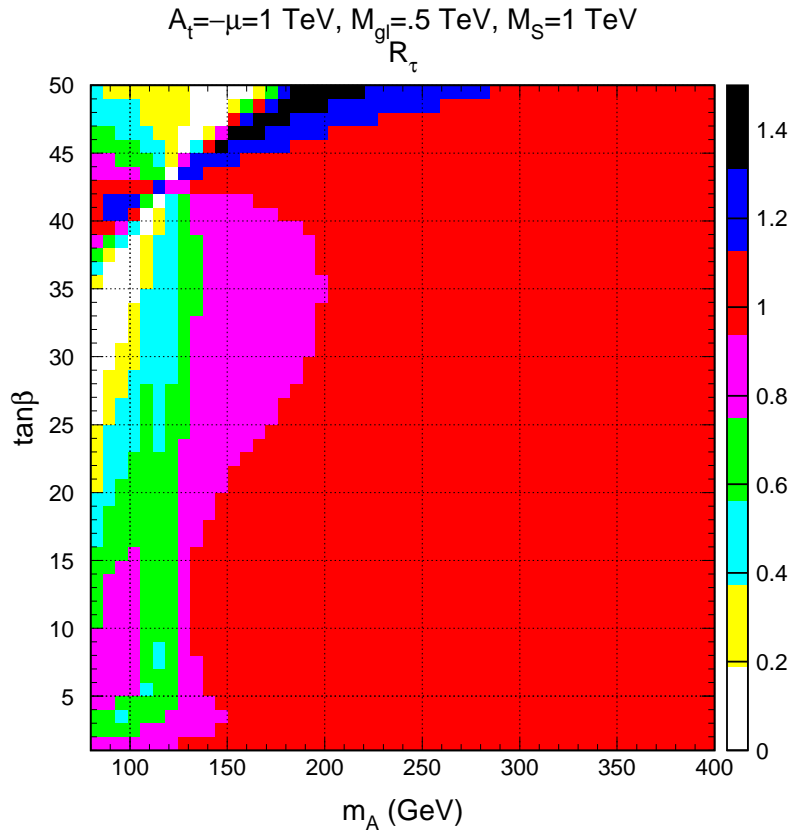
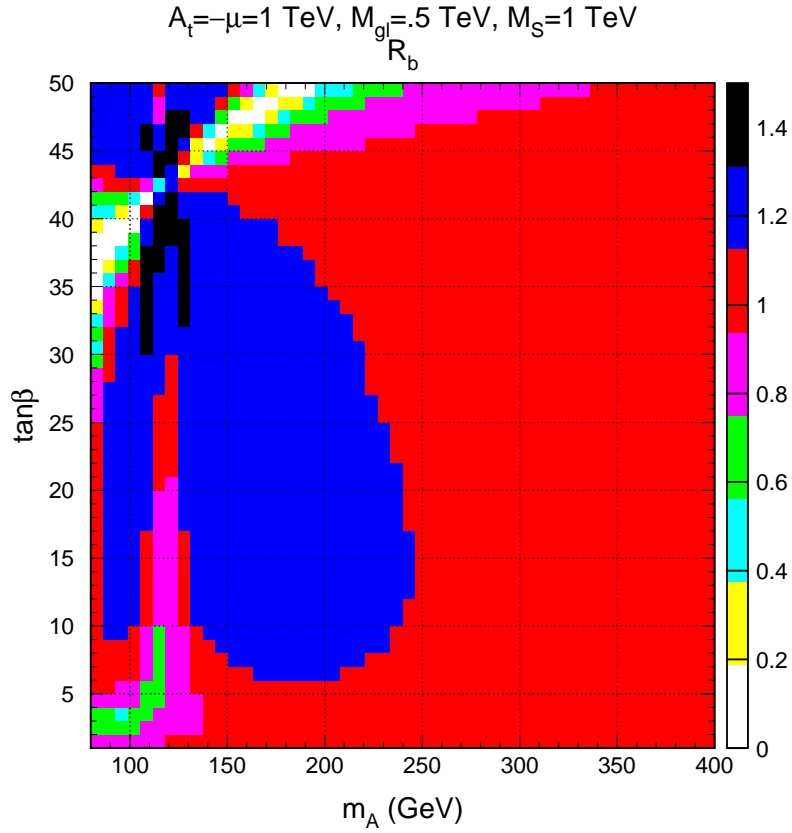


Figure 6: Comparison of the sensitivity of the $\phi_W \rightarrow b\bar{b}$ and $\phi_W \rightarrow \tau^+\tau^-$ channels, R_b and R_τ , respectively, when the Higgs ϕ_W is produced from a $VV\phi_W$ vertex, $V = W$ or Z .

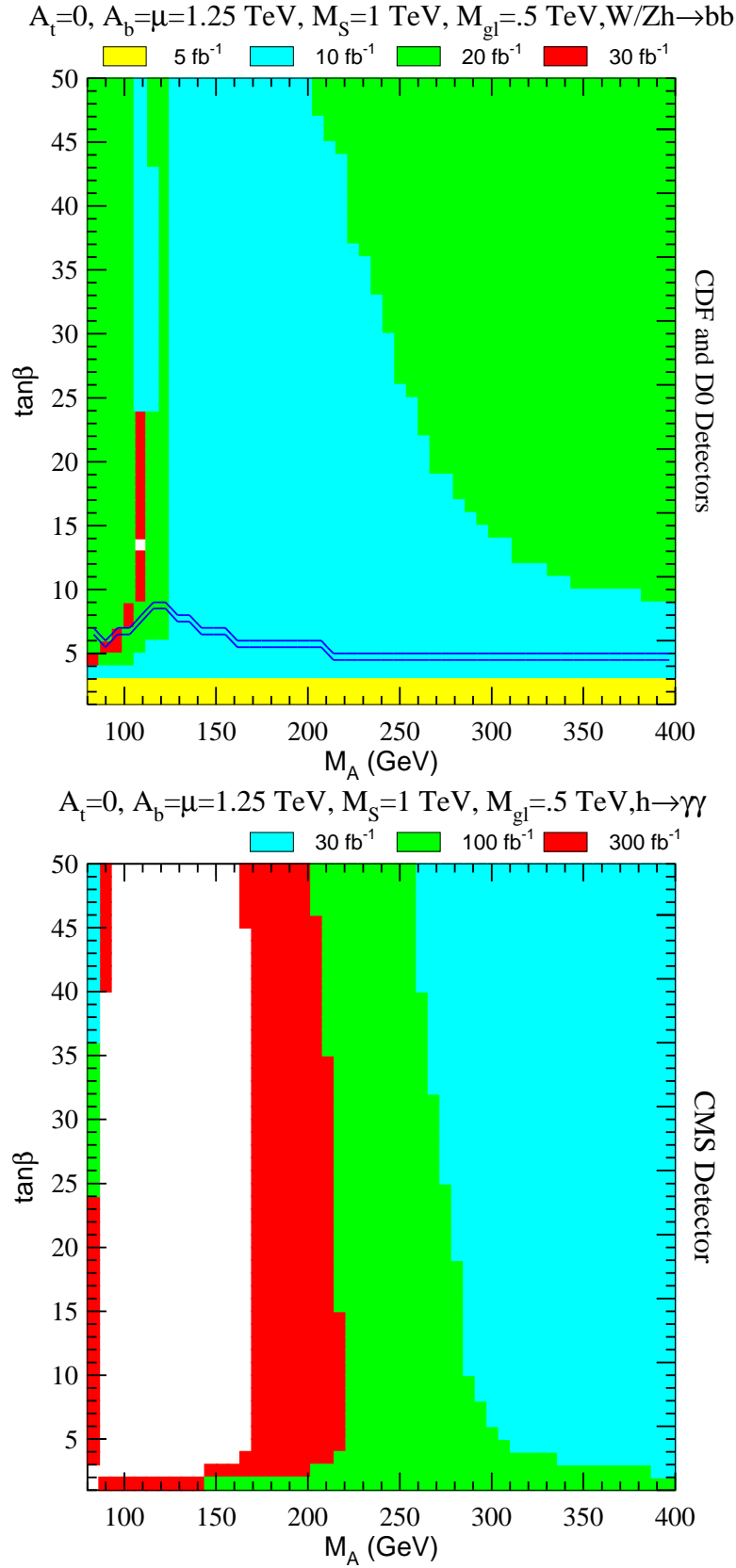
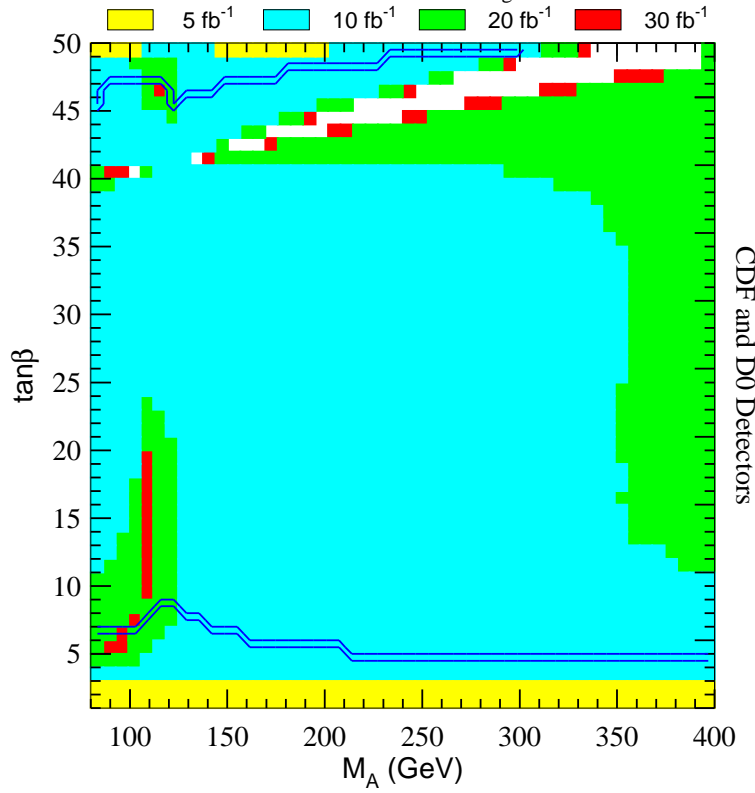


Figure 7: Same as Fig. 2, but considering a possible cancellation of $\text{BR}(\phi_W \rightarrow b\bar{b})$ for large $A_b = \mu$ and $\Delta(m_b) > 0$.

$A_t=0, A_b=\mu=1.25 \text{ TeV}, M_S=1 \text{ TeV}, M_{gl}=-.5 \text{ TeV}, W/Zh \rightarrow bb$



$A_t=0, A_b=\mu=1.25 \text{ TeV}, M_S=1 \text{ TeV}, M_{gl}=-.5 \text{ TeV}, h \rightarrow \gamma\gamma$

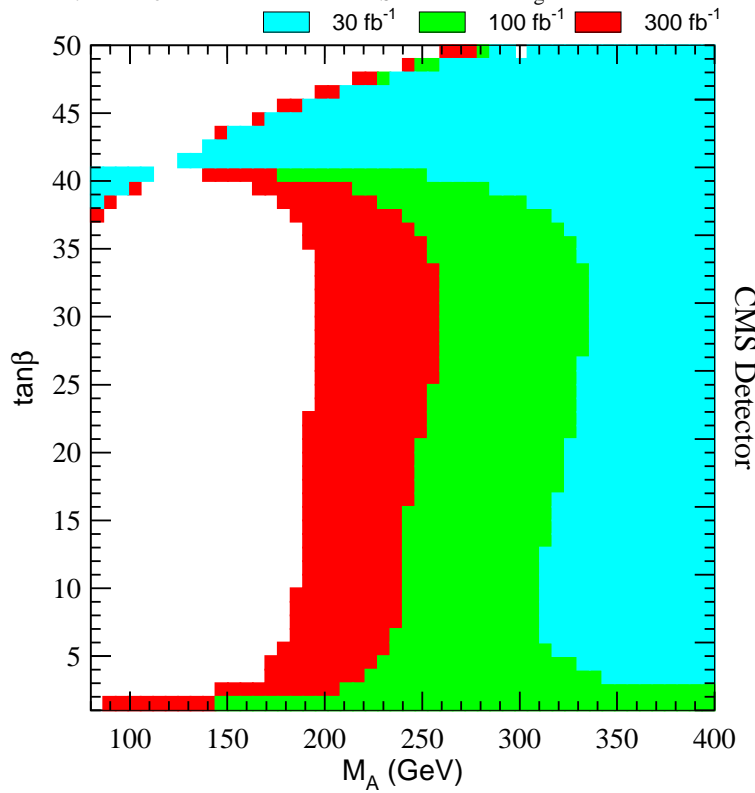


Figure 8: Same as Fig 7 but for $\Delta(m_b) < 0$.

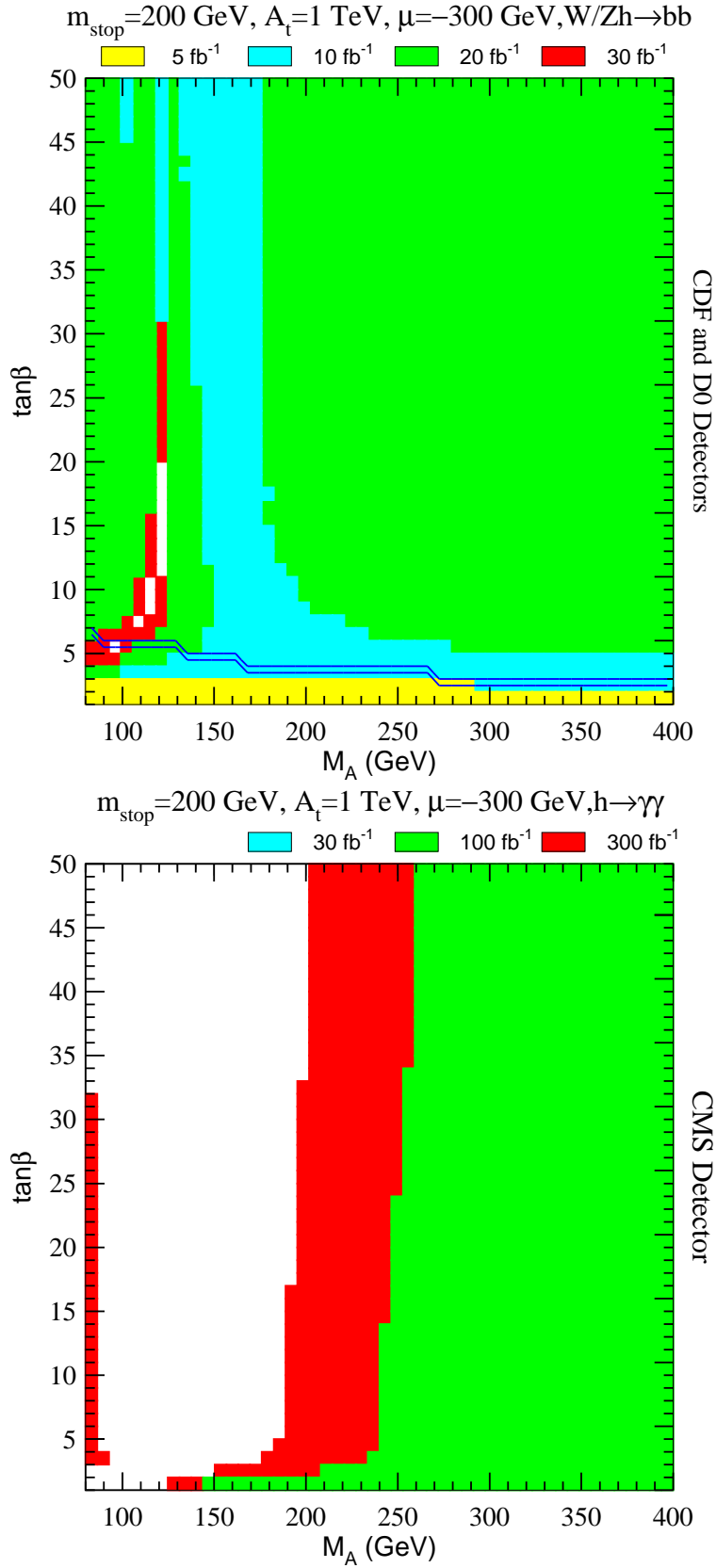


Figure 9: Same as Fig 2, but for a region of parameters such that $\Gamma(\phi_W \rightarrow gg)$ is suppressed with respect to the SM value, $M_{\tilde{t}_1} = 200 \text{ GeV}$, $A_t = 1 \text{ TeV}$, $\mu = -0.3 \text{ TeV}$

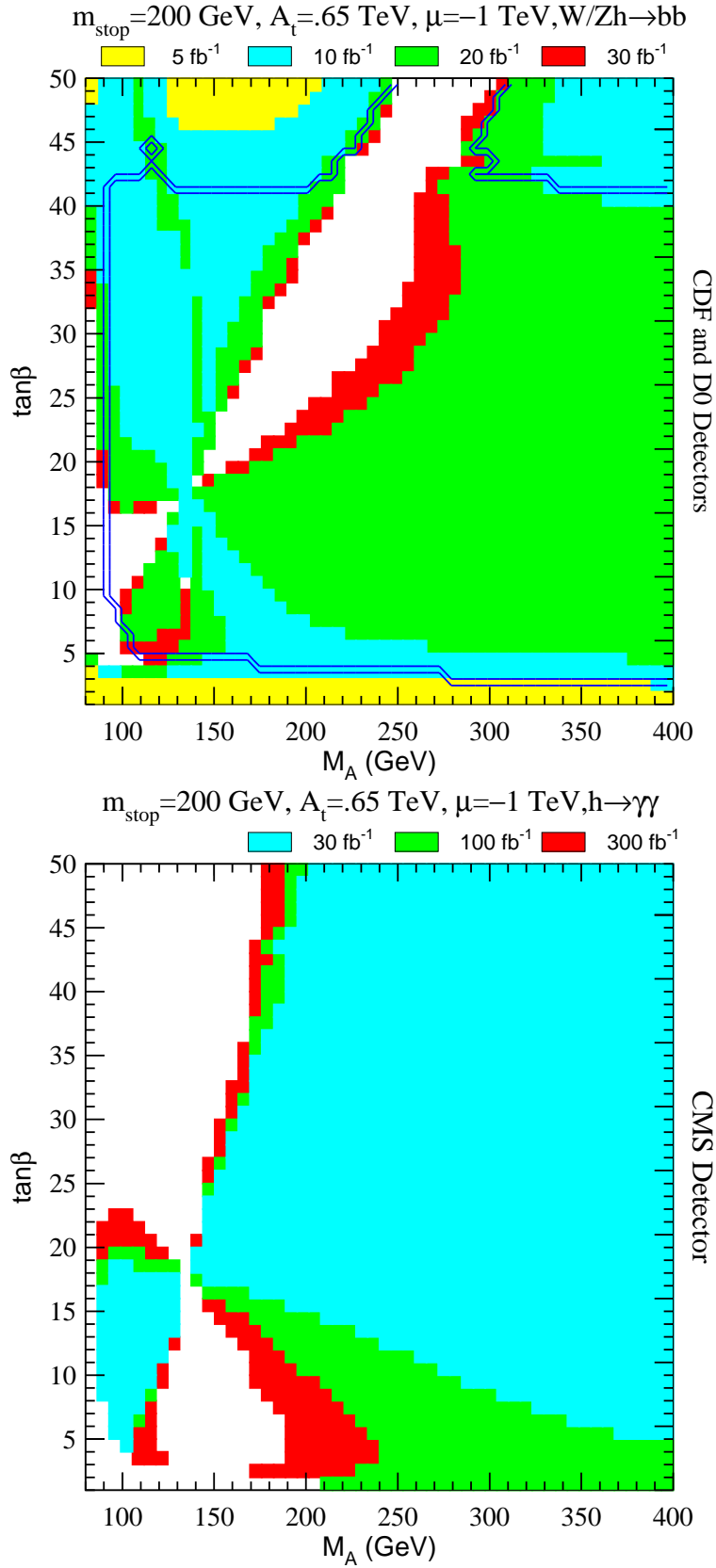


Figure 10: Same as Fig. 9, but considering stop mixing mass parameters which induce a suppression of the $\phi_W b\bar{b}$ coupling, $M_{\tilde{t}_1} = 200 \text{ GeV}$, $A_t = .65 \text{ TeV}$, $\mu = -1 \text{ TeV}$

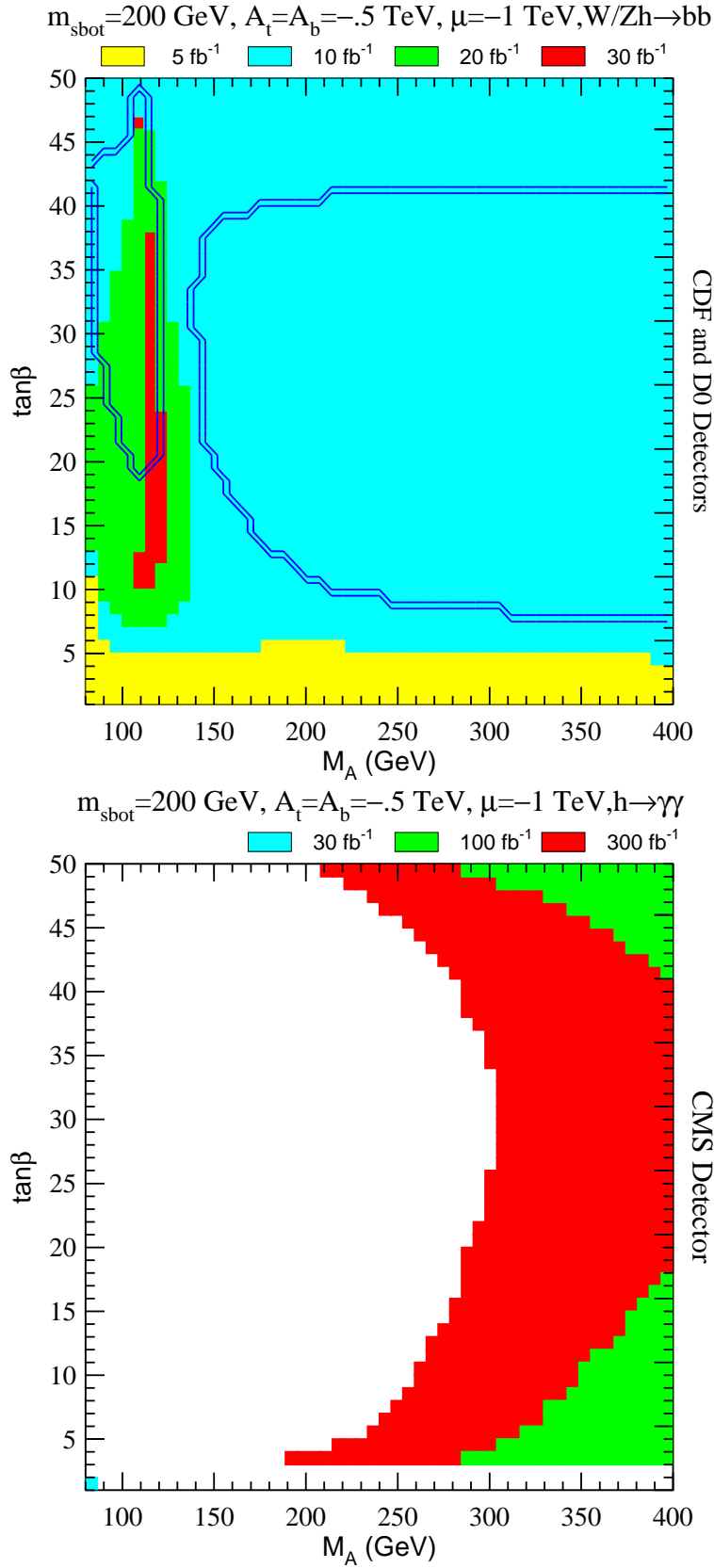


Figure 11: Same as Fig. 2, but for light top and bottom squarks, and large mixing mass parameters, $M_{\tilde{b}_1} = 200 \text{ GeV}$, $A_t = A_b = -.5 \text{ TeV}$, $\mu = -1 \text{ TeV}$